Published for SISSA by Springer

Received: June 11, 2016
Revised: September 25, 2016
Accepted: October 12, 2016
Published: October 24, 2016

Phenomenological MSSM interpretation of CMS searches in pp collisions at $\sqrt{s} = 7$ and 8 TeV

The CMS collaboration

E-mail: cms-publication-committee-chair@cern.ch

Abstract: Searches for new physics by the CMS collaboration are interpreted in the framework of the phenomenological minimal supersymmetric standard model (pMSSM). The data samples used in this study were collected at $\sqrt{s} = 7$ and 8 TeV and have integrated luminosities of 5.0 fb^{-1} and 19.5 fb^{-1}, respectively. A global Bayesian analysis is performed, incorporating results from a broad range of CMS supersymmetry searches, as well as constraints from other experiments. Because the pMSSM incorporates several well-motivated assumptions that reduce the 120 parameters of the MSSM to just 19 parameters defined at the electroweak scale, it is possible to assess the results of the study in a relatively straightforward way. Approximately half of the model points in a potentially accessible subspace of the pMSSM are excluded, including all pMSSM model points with a gluino mass below 500 GeV, as well as models with a squark mass less than 300 GeV. Models with chargino and neutralino masses below 200 GeV are disfavored, but no mass range of model points can be ruled out based on the analyses considered. The nonexcluded regions in the pMSSM parameter space are characterized in terms of physical processes and key observables, and implications for future searches are discussed.

Keywords: Hadron-Hadron scattering (experiments), Supersymmetry

ArXiv ePrint: 1606.03577

doi:10.1007/JHEP10(2016)129

Contents

JHEP10(2016)129

1 Introduction

Supersymmetry (SUSY) [1–6] is a strongly motivated candidate for physics beyond the standard model (SM). Searches for the superpartner particles (sparticles) predicted by SUSY performed in a variety of channels at the CERN LHC at $\sqrt{s} = 7$ and 8 TeV have been reported [7–18]. The results, found to be consistent with the SM, are interpreted as limits on SUSY parameters, based mostly on models with restricted degrees of freedom, such as the constrained minimal supersymmetric standard model (cMSSM) [19–25], or, more recently, within the simplified model spectra (SMS) approach [26–28]. The cMSSM models feature specific relations among the soft-breaking terms at some mediation scale that translate into specific mass patterns typical for the model. While this problem is avoided in the SMS approach, the signatures of realistic models cannot always be fully covered by SMS topologies. This holds true, for instance, in the case of long decay chains that do not correspond to any SMS, t-channel exchanges of virtual sparticles in production, or the presence of multiple production modes that overlap in kinematic distributions.

In the work reported here, data taken with the CMS experiment at the LHC are revisited with an alternative approach that is designed to assess more generally the coverage of SUSY parameter space provided by these searches. The method is based on the minimal supersymmetric standard model (MSSM) and combines several search channels and external constraints. Given the large diversity of decay modes leading to multiple signatures,

the potential benefit of such a combined limit is to exclude parameter regions that would otherwise be allowed when considering each analysis separately.

Specifically, we interpret the CMS results in terms of the phenomenological MSSM (pMSSM) [29], a 19-dimensional parametrization of the R-parity conserving, weak-scale MSSM that captures most of the latter's phenomenological features. Here, R-parity is a $\mathbb{Z}_2$ symmetry ensuring the conservation of lepton and baryon numbers [30], which suppresses proton decay and results in the lightest SUSY particle (LSP) being stable. In the pMSSM, all MSSM parameters are specified at the electroweak (EW) scale, and allowed to vary freely, subject to the requirement that the model remain consistent with EW symmetry breaking (EWSB) and other basic constraints. Since the pMSSM incorporates neither relations among SUSY-breaking terms at a high scale, nor large correlations among sparticle masses from renormalization group evolution, it allows a much broader set of scenarios than those in, for example, the cMSSM and related grand unified theories (GUTs). Many of these scenarios are difficult to constrain using current LHC data, despite some having small sparticle masses.

To assess how the data obtained by CMS impact SUSY in the context of the pMSSM, we use a representative subset of the results based on data corresponding to integrated luminosities of 5.0 fb^{-1} at 7 TeV and 19.5 fb^{-1} at 8 TeV. We use results from hadronic searches, both general searches and those targeting top squark production; also included are searches with leptonic final states, both general and EW-targeted. For a selected set of pMSSM parameter points, event samples were simulated using the CMS fast detector simulation [31] and analyzed. Since the fast detector simulation does not accurately model the detector response to massive long-lived charged particles, and since it was not feasible to use the CMS full simulation [32] given the large number of model points, we work within a subspace of the pMSSM in which the chargino proper decay lifetime $c\tau(\widetilde{\chi}^{\pm})$ is less than 10 mm. This constraint restricts the class of final states considered to those with prompt decays. The 7 and 8 TeV data are treated consistently; in particular, we use the same set of points in the pMSSM model phase space, chosen randomly from a larger set of points that are consistent with pre-LHC experimental results and basic theoretical constraints. This approach greatly facilitates the combination of the results from the 7 and 8 TeV (Run 1) data.

The statistical analysis follows closely the Bayesian approach of refs. [33, 34]. The work is an extension of ref. [35], which interpreted three independent CMS analyses based on an integrated luminosity of about 1 fb^{-1} of data [36–38] in terms of the pMSSM, confirming that the approach is both feasible and more successful in yielding general conclusions about SUSY than those based on constrained SUSY models. Furthermore, the diversity of phenomena covered by the pMSSM is also helpful in suggesting new approaches to searches for SUSY at the LHC. A similar study has been performed by the ATLAS experiment [39].

The paper is organized as follows. The definition of the pMSSM is presented in section 2. Section 3 describes the analysis, which includes the construction of a statistical prior for the pMSSM model and the calculation of likelihoods for the CMS searches. The results of this study are presented in section 4, including discussions of the impact of the Run 1 CMS searches and their current sensitivity to the pMSSM. Section 5 discusses nonexcluded pMSSM phase space. A summary of the results is given in section 6.

JHEP10(2016)129

2 Definition of the phenomenological MSSM

The weak-scale R-parity conserving MSSM [29] has 120 free parameters, assuming the gravitino is heavy. This is clearly too large a parameter space for any phenomenological study. However, most of these parameters are associated with CP-violating phases and/or flavor changing neutral currents (FCNC), which are severely constrained by experiment. Therefore, a few reasonable assumptions about the flavor and CP structure allow a factor of six reduction in the number of free parameters, without imposing any specific SUSY breaking mechanism. This has the virtue of avoiding relations, which need not hold in general, between the soft terms introduced by models of SUSY breaking.

Strong constraints on CP violation are satisfied by taking all parameters to be real, and FCNC constraints are satisfied by taking all sfermion mass matrices and trilinear couplings to be diagonal in flavor. Moreover, the first two generations of sfermions are assumed to be degenerate. The trilinear A-terms of the first two generations give rise to amplitudes that are proportional to very small Yukawa couplings and are thus not experimentally relevant. Only the third generation parameters A_{t}, A_{b}, and A_τ have consequences that are potentially observable.

This leaves 19 real weak-scale SUSY Lagrangian parameters that define the pMSSM [29]. As noted above, the pMSSM captures most of the phenomenological features of the R-parity conserving MSSM and, most importantly, encompasses and goes beyond a broad range of more constrained SUSY models. In addition to the SM parameters, the free parameters of the pMSSM are:

- three independent gaugino mass parameters M_1, M_2, and M_3,
- the ratio of the Higgs vacuum expectation values $\tan\beta = v_2/v_1$,
- the higgsino mass parameter μ and the pseudoscalar Higgs boson mass m_A,
- 10 independent sfermion mass parameters $m_{\tilde{\mathrm{F}}}$, where $\tilde{\mathrm{F}} = \tilde{\mathrm{Q}}_1$, $\tilde{\mathrm{U}}_1$, $\tilde{\mathrm{D}}_1$, $\tilde{\mathrm{L}}_1$, $\tilde{\mathrm{E}}_1$, $\tilde{\mathrm{Q}}_3$, $\tilde{\mathrm{U}}_3$, $\tilde{\mathrm{D}}_3$, $\tilde{\mathrm{L}}_3$, $\tilde{\mathrm{E}}_3$ (for the 2nd generation we take $m_{\tilde{\mathrm{Q}}_2} \equiv m_{\tilde{\mathrm{Q}}_1}$, $m_{\tilde{\mathrm{L}}_2} \equiv m_{\tilde{\mathrm{L}}_1}$, $m_{\tilde{\mathrm{U}}_2} \equiv m_{\tilde{\mathrm{U}}_1}$, $m_{\tilde{\mathrm{D}}_2} \equiv m_{\tilde{\mathrm{D}}_1}$, and $m_{\tilde{\mathrm{E}}_2} \equiv m_{\tilde{\mathrm{E}}_1}$; left-handed up- and down-type squarks are by construction mass degenerate), and
- the trilinear couplings A_{t}, A_{b} and A_τ.

To minimize theoretical uncertainties in the Higgs sector, these parameters are conveniently defined at a scale equal to the geometric mean of the top squark masses, $M_{\mathrm{SUSY}} \equiv \sqrt{m_{\tilde{\mathrm{t}}_1} m_{\tilde{\mathrm{t}}_2}}$, often also referred to as the EWSB scale.

The pMSSM parameter space is constrained by a number of theoretical requirements. First, the sparticle spectrum must be free of tachyons (particles with negative physical mass) and cannot lead to color or charge breaking minima in the scalar potential. We also require that EWSB be consistent and that the Higgs potential be bounded from below. Finally, in this study, we also require that the lightest SUSY particle (LSP) be the lightest neutralino, $\widetilde{\chi}_1^0$. These requirements yield a model that is an excellent proxy for the full MSSM with few enough parameters that an extensive exploration is possible.

JHEP10(2016)129

It is of interest to note the generic properties of sparticle mass spectra of the pMSSM. By definition, each first generation sfermion is exactly degenerate in mass with the corresponding second generation sfermion. Other generic properties of pMSSM mass spectra are actually MSSM properties; in the first and second generations, spartners of left-handed down-type quarks are nearly mass-degenerate with the corresponding up-type squarks. Likewise, first and second generation spartners of left-handed charged leptons are nearly degenerate with the corresponding sneutrinos. The nature of the spectrum of neutralinos and charginos depends on the relative magnitudes and separation of the pMSSM parameters M_1, M_2 and μ. If these scales are well separated, then the approximate eigenstates will divide into a single bino-like state with mass of order M_1, a wino-like triplet consisting of two charginos and one neutralino with masses of order M_2, and a higgsino-like quartet of two charginos and two neutralinos with masses of order μ. The LSP will then be primarily composed of the neutral member(s) of the lightest of these three. If the parameters above are not well separated, then the LSP will be a mixture of the neutral states.

3 Analysis

The purpose of this work is to assess how the current data constrain the MSSM using the more tractable pMSSM as a proxy. We use the results from several CMS analyses, which cover a variety of final states, to construct posterior densities of model parameters, masses, and observables. The posterior density of the model parameters, which are denoted by θ, is given by

$$p(\theta|D^{\mathrm{CMS}}) \propto L(D^{\mathrm{CMS}}|\theta)\, p^{\text{non-DCS}}(\theta), \tag{3.1}$$

where D^{CMS} denotes the data analyzed by the direct CMS SUSY searches, $L(D^{\mathrm{CMS}}|\theta)$ is the associated CMS likelihood that incorporates the impact of these direct CMS searches, and $p^{\text{non-DCS}}(\theta)$ is the prior density constructed from results not based on direct CMS SUSY searches (non-DCS results). The posterior density for an observable λ is obtained as follows,

$$p(\lambda|D^{\mathrm{CMS}}) = \int \delta[\lambda - \lambda'(\theta)]\, p(\theta|D^{\mathrm{CMS}})\, \mathrm{d}\theta, \tag{3.2}$$

where $\lambda'(\theta)$ is the value of the observable as predicted by model point θ (θ identifies the model point). Equation (3.2) is approximated using Monte Carlo (MC) integration. In the following, we describe the construction of the prior density and CMS likelihoods.

3.1 Construction of the prior

If the posterior density for a given parameter differs significantly from its prior density (or prior, for short), then we may conclude that the data have provided useful information about the parameter; otherwise, the converse is true. However, for such conclusions to be meaningful, it is necessary to start with a prior that encodes as much relevant information as possible. In this study, the prior $p^{\text{non-DCS}}(\theta)$ encodes several constraints: the parameter space boundary, several theoretical conditions, the chargino lifetimes, and most importantly the constraints from non-DCS data, such as precision measurements and pre-LHC new physics searches. We choose not to include data from dark matter (DM) experiments in

JHEP10(2016)129

the prior, which avoids any bias from cosmological assumptions (e.g., DM density and distribution, assumption of one thermal relic, no late entropy production, etc.).

The prior $p^{\text{non-DCS}}(\theta)$ is formulated as a product of four factors,

$$p^{\text{non-DCS}}(\theta) \propto \left[\prod_j L(D_j^{\text{non-DCS}}|\lambda_j(\theta))\right] \; p\big(c\tau(\widetilde{\chi}^{\pm})<10\,\text{mm}\,|\theta\big) \;\; p(\text{theory}|\theta) \;\; p_0(\theta). \quad (3.3)$$

The initial prior $p_0(\theta)$ is taken to be uniform in the pMSSM subspace,

$$\begin{aligned} -3 \leq \;& M_1, M_2 \leq 3\,\text{TeV}, \\ 0 \leq \;& M_3 \leq 3\,\text{TeV}, \\ -3 \leq \;& \mu \leq 3\,\text{TeV}, \\ 0 \leq \;& m_{\text{A}} \leq 3\,\text{TeV}, \\ 2 \leq \;& \tan\beta \leq 60, \\ 0 \leq m_{\tilde{\text{Q}}_{1,2}}, m_{\tilde{\text{U}}_{1,2}}, m_{\tilde{\text{D}}_{1,2}}, & m_{\tilde{\text{L}}_{1,2}}, m_{\tilde{\text{E}}_{1,2}}, m_{\tilde{\text{Q}}_3}, m_{\tilde{\text{U}}_3}, m_{\tilde{\text{D}}_3}, m_{\tilde{\text{L}}_3}, m_{\tilde{\text{E}}_3} \leq 3\,\text{TeV}, \\ -7 \leq \;& A_{\text{t}}, A_{\text{b}}, A_\tau \leq 7\,\text{TeV}, \end{aligned} \quad (3.4)$$

and the formally unbounded SM subspace defined by m_{t}, $m_{\text{b}}(m_{\text{b}})$, and $\alpha_{\text{s}}(m_{\text{Z}})$; the non-DCS measurements, which are listed in table 1, constrain these parameters within narrow ranges. A point in this subspace is denoted by θ. The subspace defined in eqs. (3.4) covers the phenomenologically viable parameter space for the LHC and is large enough to cover sparticle masses to which the LHC might conceivably be ultimately sensitive. The lower bound of 2 for $\tan\beta$ evades non-perturbative effects in the top-quark Yukawa coupling after evolution up to the GUT scale. These effects typically become a very serious issue for $\tan\beta \lesssim 1.7$ [40]. The term $p(\text{theory}|\theta)$ imposes the theoretical constraints listed at the end of section 2, while $p(c\tau(\widetilde{\chi}^{\pm}) < 10\,\text{mm}|\theta)$ imposes the prompt chargino constraint. Both $p(\text{theory}|\theta)$ and $p(c\tau(\widetilde{\chi}^{\pm}) < 10\,\text{mm}|\theta)$ are unity if the inequalities are satisfied and zero otherwise.

The product of likelihoods $L(D^{\text{non-DCS}}|\lambda(\theta))$ in eq. (3.3) over measurements j is associated with non-DCS data $D^{\text{non-DCS}}$, which imposes constraints from precision measurements and a selection of pre-LHC searches for new physics. The measurements used and their associated likelihoods are listed in table 1.

Since the explicit functional dependence of the prior $p^{\text{non-DCS}}(\theta)$ on θ is not available *a priori*, but the predictions $\lambda(\theta)$ are available point by point, it is natural to represent the prior as a set of points sampled from it. Owing to the complexity of the parameter space, the sampling is performed using a Markov chain Monte Carlo (MCMC) method [34, 41–44].

All data in table 1 except the Higgs boson signal strengths μ_{h} were used in the original MCMC scan. The μ_{h} measurements were incorporated into the prior post-MCMC. A number of measurements, marked "reweight" in the last column, were updated during the course of this study as new results became available. The weights, applied to the subset of scan points which were selected for simulation, were computed as the likelihood ratio of the new measurements shown in table 1 to the previously available measurements.

JHEP10(2016)129

i	Observable $\mu_i(\theta)$	Constraint $D_i^{\text{non-DCS}}$	Likelihood function $L[D_i^{\text{non-DCS}}\|\mu_i(\theta)]$	Comment
1	$\mathcal{B}(\mathrm{b} \to \mathrm{s}\gamma)$ [45]	$(3.43 \pm 0.21^{\text{stat}} \pm 0.24^{\text{th}} \pm 0.07^{\text{sys}}) \times 10^{-4}$	Gaussian	reweight
2	$\mathcal{B}(\mathrm{B_s} \to \mu\mu)$ [46]	$(2.9 \pm 0.7 \pm 0.29^{\text{th}}) \times 10^{-9}$	Gaussian	reweight
3	$R(\mathrm{B} \to \tau\nu)$ [45, 47]	1.04 ± 0.34	Gaussian	reweight
4	Δa_μ [48]	$(26.1 \pm 6.3^{\text{exp}} \pm 4.9^{\text{SM}} \pm 10.0^{\text{SUSY}}) \times 10^{-10}$	Gaussian	
5	$\alpha_{\mathrm{s}}(m_{\mathrm{Z}})$ [49]	0.1184 ± 0.0007	Gaussian	
6	m_{t} [50]	$173.20 \pm 0.87^{\text{stat}} \pm 1.3^{\text{sys}}$ GeV	Gaussian	reweight
7	$m_{\mathrm{b}}(m_{\mathrm{b}})$ [49]	$4.19^{+0.18}_{-0.06}$ GeV	Two-sided Gaussian	
8	m_{h}	LHC: $m_{\mathrm{h}}^{\text{low}} = 120$ GeV, $m_{\mathrm{h}}^{\text{high}} = 130$ GeV	1 if $m_{\mathrm{h}}^{\text{low}} \le m_{\mathrm{h}} \le m_{\mathrm{h}}^{\text{high}}$ 0 if $m_{\mathrm{h}} < m_{\mathrm{h}}^{\text{low}}$ or $m_{\mathrm{h}} > m_{\mathrm{h}}^{\text{high}}$	reweight
9	μ_{h}	CMS and ATLAS in LHC Run 1, Tevatron	LILITH 1.01 [51, 52]	post-MCMC
10	sparticle masses	LEP [53] (via MICROMEGAS [54–56])	1 if allowed 0 if excluded	

Table 1. The measurements that form the basis of the non-DCS prior $p^{\text{non-DCS}}(\theta)$ for the pMSSM parameters, their observed values and likelihoods. The observables are the decay branching fractions $\mathcal{B}(\mathrm{b} \to \mathrm{s}\gamma)$ and $\mathcal{B}(\mathrm{B_s} \to \mu\mu)$, the ratio of the measured branching fraction of the decay $\mathrm{B} \to \tau\nu$ to that predicted by the standard model, $R(\mathrm{B} \to \tau\nu)$, the difference in the muon anomolous magnetic moment from its SM prediction Δa_μ, the strong coupling constant at the Z boson mass $\alpha_{\mathrm{s}}(m_{\mathrm{Z}})$, the top and bottom quark masses m_{t} and $m_{\mathrm{b}}(m_{\mathrm{b}})$, the Higgs boson mass m_{h} and signal strength μ_{h}, and sparticle mass limits from LEP. All data except μ_{h} were used in the initial MCMC scan. Details are given in the text.

For a given point θ, the predictions $\lambda(\theta)$ — including those needed to calculate the likelihoods $L(D^{\text{non-DCS}}|\lambda(\theta))$ — are obtained as follows. The physical masses and interactions are calculated using the SUSY spectrum generator SOFTSUSY 3.3.1 [57], with the input parameters θ defined at M_{SUSY}. This calculation includes 1-loop corrections for sparticle masses and mixings, as well as 2-loop corrections for the small Higgs boson mass. Low-energy constraints are calculated with SUPERISO v3.3 [58]. MICROMEGAS 2.4.5 [54–56] is used to check the compatibility of pMSSM points with sparticle mass limits from LEP and other pre-LHC experiments. MICROMEGAS is also used to compute the DM relic density, and the spin-dependent and spin-independent DM-nucleon scattering cross sections; these observables are not used in the construction of the prior, but we study how they are impacted by the CMS searches. The program SDECAY 1.3 [59] is used to generate sparticle decay tables and HDECAY 5.11 [60] to generate Higgs boson decay tables. For evaluating the Higgs boson signal likelihood based on the latest ATLAS [61] and CMS [62] measurements, we use LILITH 1.01 [51, 52], following the approach explained in section 2.3 of ref. [63]. The experimental results used in LILITH are the signal strengths of the Higgs boson decay modes $Y = (\gamma\gamma,\ \mathrm{WW}^*,\ \mathrm{ZZ}^*,\ \mathrm{b\bar{b}}, \tau\tau)$ in terms of the primary Higgs boson production modes gluon-gluon fusion (ggF), vector boson fusion (VBF), associated production with a W or Z boson (Wh and Zh, commonly denoted as Vh), and associated production with a top-quark pair ($\mathrm{t\bar{t}h}$) as published by ATLAS, CMS, and Tevatron experiments. When these signal strengths are given as 2-dimensional (2D) confidence level (CL) contours in, e.g., the $\mu_{\text{ggF+tth}}(Y)$ versus $\mu_{\text{VBF+Vh}}(Y)$ plane, the likelihood is reconstructed by fitting a 2D Gaussian function to the 68% CL contour provided by the experiments. For each experiment,

JHEP10(2016)129

the likelihood is then given by $-2\log L_Y = \chi^2_Y$ for each decay mode Y, and the combined likelihood is then obtained by summing over all the individual χ^2_Y values. Additional information on signal strengths (and invisible decays) in one dimension is included analogously, using the published likelihood function when available or else the Gaussian approximation.

The uncertainty in the anomalous magnetic moment of the muon includes a component that accounts for theoretical uncertainties in the SUSY calculations.

The large window on the Higgs boson mass of 120–130 GeV covers the theoretical uncertainty in the Higgs boson mass calculation in the MSSM. All tools use the SUSY Les Houches accord [64] for data entry and output. Approximately 20 million points are sampled from $p^{\text{non-DCS}}(\theta)$ using multiple MCMC chains, but omitting the prompt chargino requirement. When that requirement is imposed, the number of sampled points is reduced by 30%, and the fraction of bino-like LSPs is enhanced from about 40 to 50%. A random subsample of 7200 points is selected for simulation studies. Given the large dimensionality of the model, this is a rather sparse scan. However, the scan density is sufficient to learn much about the viability of the pMSSM model space. Distributions of model parameters in this subsample were compared with distributions from independent subsamples of similar size, as well as distributions from the original large sample, and consistency was observed within statistical uncertainties.

3.2 Incorporation of the CMS data

We consider the analyses given in table 2, which explore final-state topologies characterized by a variety of event-level observables: the scalar sum of the transverse momenta of jets (H_{T}); the magnitude of the vector sum of the transverse momenta of final-state particles ($E_{\text{T}}^{\text{miss}}$ or $H_{\text{T}}^{\text{miss}}$); a measure of the transverse mass in events with two semi-invisibly decaying particles (M_{T2}); the multiplicity of b-tagged jets (b-jets); and a range of lepton multiplicities, including opposite-sign (OS) and like-sign (LS) lepton pairs. Other analyses that were not included in this study but which may impose additional constraints on the model space include searches for SUSY in the single lepton channel with one or multiple b-jets [65] and searches for top squark production [66] in the single lepton channel. The searches considered together comprise hundreds of signal regions and address a large diversity of possible signal topologies.

The CMS likelihoods $L(D^{\text{CMS}}|\theta)$ are calculated for each of these analyses (or combinations of analyses), using different forms of likelihood depending on the nature of the results that are available. The first form of likelihood (*counts*) uses observed counts, N, and associated background estimates, $B \pm \delta B$; the second (χ^2) uses profile likelihoods, $T(\mu, \theta)$, where $\mu = \sigma/\sigma^{\text{SUSY}}(\theta)$ is the signal strength modifier and σ and $\sigma^{\text{SUSY}}(\theta)$ are the observed and predicted SUSY cross sections, respectively; while the third (*binary*) joins either of the first two kinds of result together with a signal significance measure Z, and is used for combining results from overlapping search regions. In the following, we describe the three forms of the likelihood used and the signal significance measure Z.

JHEP10(2016)129

Analysis	$\sqrt{s}$ [TeV]	$\mathcal{L}$ [fb^{-1}]	Likelihood
Hadronic $H_T + H_T^{miss}$ search [8]	7	4.98	counts
Hadronic $H_T + E_T^{miss}$ + b-jets search [9]	7	4.98	counts
Leptonic search for EW prod. of $\widetilde{\chi}^0$, $\widetilde{\chi}^{\pm}$, $\tilde{l}$ [10]	7	4.98	counts
Hadronic $H_T + H_T^{miss}$ search [11]	8	19.5	counts
Hadronic M_{T2} search [12]	8	19.5	counts
Hadronic $H_T + E_T^{miss}$ + b-jets search [13]	8	19.4	χ^2
Monojet searches [14]	8	19.7	binary
Hadronic third generation squark search [15]	8	19.4	counts
OS dilepton (OS ll) search [16] (counting experiment only)	8	19.4	counts
LS dilepton (LS ll) search [17] (only channels w/o third lepton veto)	8	19.5	counts
Leptonic search for EW prod. of $\widetilde{\chi}^0$, $\widetilde{\chi}^{\pm}$, $\tilde{l}$ [18] (only LS, 3 lepton, and 4 lepton channels)	8	19.5	counts
Combination of 7 TeV searches	7	—	binary
Combination of 7 and 8 TeV searches	7, 8	—	binary

Table 2. The CMS analyses considered in this study. Each row gives the analysis description, the center-of-mass energy at which data were collected, the associated integrated luminosity, the likelihood used, and the reference to the analysis documentation.

Counts likelihood. For a single-count analysis, the likelihood is given by

$$L(D^{\mathrm{CMS}}|\theta) = \int \mathrm{Poisson}(N|s(\theta)+b)\, p(b|B,\delta B)\mathrm{d}b, \tag{3.5}$$

where N is the observed count, $s(\theta)$ and b are the expected number of signal and background counts, respectively, and $B \pm \delta B$ is the estimated number of background event counts and its uncertainty. The prior density for b, $p(b|B,\delta B)$, is modeled as a gamma density, $\mathrm{gamma}(x;\alpha,\beta) = \beta \exp(-\beta x)(\beta x)^{\alpha-1}/\Gamma(\alpha)$, with α and β defined such that the mode and variance of the gamma density are B and $(\delta B)^2$, respectively. For analyses that yield multiple independent counts, the likelihood is the product of the likelihoods of the individual counts. For analyses with multiple counts, we treat the background predictions for the different search regions as uncorrelated. Systematic effects on the signal counts are taken into account by varying the signal yield by multiplying it with a signal strength modifier μ with values $1-\delta\mu, 1, 1+\delta\mu$, where $\delta\mu$ is the fractional value of the systematic uncertainty.

χ^2 likelihood. This likelihood is used for CMS searches that provide profile likelihoods, $T(\mu,\theta) \equiv L(D^{\mathrm{CMS}}|\mu,\theta,\hat{\nu}(\mu,\theta))$, for the signal strength modifier μ, where ν represents the nuisance parameters and $\hat{\nu}(\mu,\theta)$ their conditional maximum likelihood estimates. Taking $\hat{\mu}$ to be the signal strength modifier that maximizes $T(\mu,\theta)$, it can be shown that the

JHEP10(2016)129

quantity $t = -2\ln[T(1,\theta)/T(\hat{\mu},\theta)]$ follows a χ^2 density with one degree of freedom in the asymptotic limit [67],

$$L(D^{\mathrm{CMS}}|\theta) = \exp(-t/2)/\sqrt{2\pi t}, \tag{3.6}$$

which we adopt as the CMS likelihood in this case. The systematic uncertainties in the signal yield can again be incorporated by varying the value of μ.

***Z*-significance.** This study uses a signal significance measure defined by

$$Z(\theta) = \mathrm{sign}[\ln B_{10}(D,\theta)]\sqrt{2|\ln B_{10}(D,\theta)|}, \tag{3.7}$$

where

$$B_{10}(D,\theta) = \frac{L(D|\theta,H_1)}{L(D|H_0)} \tag{3.8}$$

is the local Bayes factor for data D, at point θ, and $L(D|\theta,H_1)$ and $L(D|H_0)$ are the likelihoods for the signal plus background (H_1) and background only (H_0) hypotheses, respectively. The function $Z(\theta)$ is a signed Bayesian analog of the frequentist "n-sigma". The case $Z \gg 0$ would indicate the presence of a signal at a significance of Z standard deviations, while the case $Z \ll 0$ would indicate the absence of signal, i.e., an *exclusion* at a significance of Z standard deviations. The Z-significance is the basis of the binary likelihood.

Binary likelihood. This likelihood is used for combining results from search regions in which data may not be independent, for example, multiple counts from overlapping search regions. We first divide the data into subsets for which either a count or χ^2 likelihood can be calculated. For each subset j, with data D_j, we compute $Z_j(\theta)$ using eq. (3.7). An overall significance measure that includes all subsets under consideration is defined by

$$Z(\theta) \equiv Z_{j_{\max}}(\theta), \tag{3.9}$$

where $j_{\max}$ is the index of the maximum element in the set $\{|Z_j(\theta)|\}$. This quantity is used to define the binary likelihood as follows,

$$L(D^{\mathrm{CMS}}|\theta) = \begin{cases} 1 & \text{if } Z(\theta) > -1.64, \\ 0 & \text{if } Z(\theta) \leq -1.64, \end{cases} \tag{3.10}$$

where $Z(\theta) = -1.64$ corresponds to the frequentist threshold for exclusion at the 95% CL. Systematic uncertainties are incorporated by computing each $Z_j(\theta)$ by varying the value of μ, and using these recalculated $Z_j(\theta)$ to compute the binary likelihood. Although use of the binary likelihood entails a loss of information, it is a convenient approach in cases of non-disjoint data, where a proper likelihood calculation is not feasible without more information. In this study, we use binary likelihoods for monojet searches, which have overlapping search regions, and for combining the 7 TeV, and 7+8 TeV results, where the considered analyses use nondisjoint data.

To compute likelihoods and Z-significances, expected signal counts for the search regions of each analysis are computed for the 7200 pMSSM points. The simulated events for each model point, which were generated using PYTHIA 6.4 [68] and processed with the CMS fast detector simulation program [31], are passed through the analysis procedures in order to determine the counts. For each pMSSM point, 10,000 events have been simulated.

JHEP10(2016)129

4 Results

We present the results of our study using three different approaches to assess the implications of the analyses for the pMSSM parameter space. In the first approach, we compare the distributions of the Z-significances. In the second approach, we compare the prior and posterior densities of the pMSSM parameters. In the third approach, we use a measure of the parameter space that remains after inclusion of the CMS search results. This measure, the survival probability in a region Θ of the pMSSM parameter space, is defined by

$$\frac{\int_\Theta p^{\text{non-DCS}}(\theta) H(Z(\theta) + 1.64) \mathrm{d}\theta}{\int_\Theta p^{\text{non-DCS}}(\theta)\, \mathrm{d}\theta}, \tag{4.1}$$

where H is the Heaviside step function with a threshold value $Z = -1.64$, which again is the threshold for exclusion at the 95% CL.

4.1 Global significance

Distributions of Z-significance are shown in figure 1 for all the CMS searches included in this study: 8 TeV searches, combinations of 7 TeV searches, and combinations of 7+8 TeV searches. The farther a Z distribution is from zero, the greater the impact of the analysis on the pMSSM parameter space. As noted in section 3, negative and positive values indicate a preference for the background only (H_0) and the signal plus background (H_1) hypotheses, respectively.

All 8 TeV searches lead to distributions with negative tails, indicating that each disfavors some region of the parameter space. The searches making the greatest impact are the H_{T}+$H_{\mathrm{T}}^{\mathrm{miss}}$ and M_{T2} searches, which disfavor a significant portion of the parameter space. The M_{T2}, H_{T}+$E_{\mathrm{T}}^{\mathrm{miss}}$+b-jets, EW, and OS dilepton searches, which yield modest excesses over the SM predictions, have Z-significances up to 4.

As expected, the combined 7+8 TeV result has a greater impact than any individual analysis. Overall, the impact of the 7 TeV combined result is relatively small as indicated by the high peak around zero. The dip around zero in the combined 7+8 TeV distribution arises from the way we combine Z-significances. As expressed in eq. (3.9), the maximum Z-significance values are used in the combination.

4.2 Impact on parameters

Figure 2 shows the impact of the CMS searches on our knowledge of the gluino mass. Figures 2 (top left, top right and bottom left) show marginalized distributions of the gluino mass. Posterior distributions obtained using three signal strength modifier values $\mu = 0.5, 1.0, 1.5$ illustrate the effect of a $\pm 50\%$ systematic uncertainty in the predicted SUSY signal yields. Since the uncertainty in the signal efficiency typically varies between 10 and 25%, and the uncertainty in the signal cross section ranges between 30 and 50%, this prescription is considered to be conservative. Figure 2 (top-left) shows the strong impact of the inclusive analyses on the gluino mass distribution. The H_{T}+$H_{\mathrm{T}}^{\mathrm{miss}}$ search strongly disfavors the region below 1200 GeV, while the M_{T2} search leads to a distribution with two regions of peaking probability, one at relatively low mass, around 600 to 1000 GeV, and one above

JHEP10(2016)129

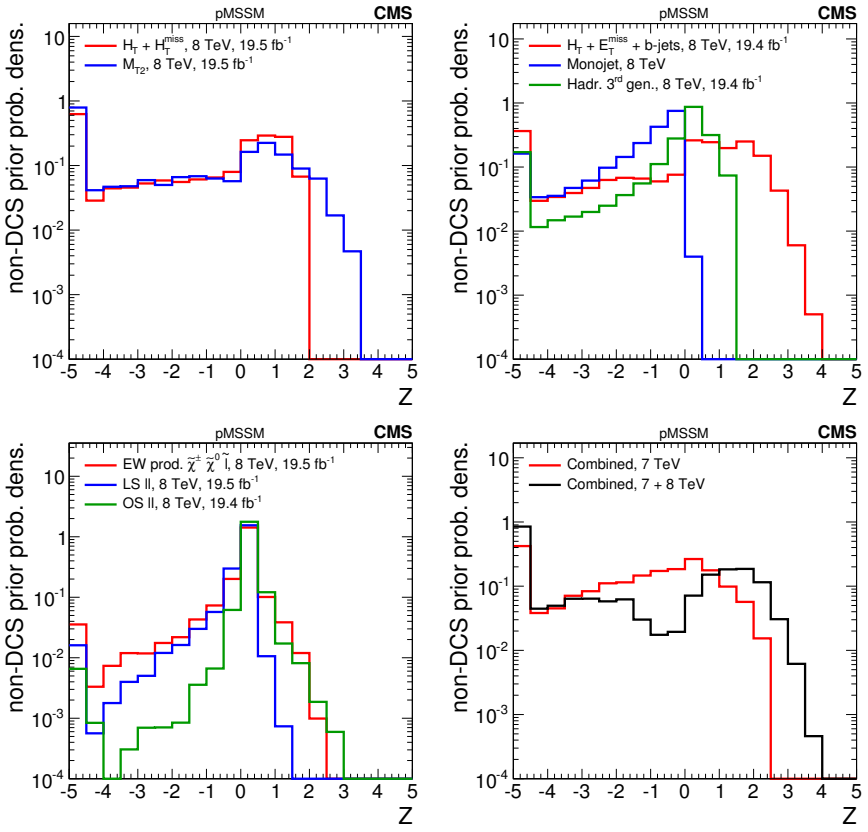

Figure 1. The distribution of the Z-significance of model points, weighted by the non-DCS prior density of each model point, for the individual 8 TeV searches (top left, top right and bottom left), and for 7 TeV combined and 7+8 TeV combined searches (bottom right). The leftmost bins contain the underflow entries.

1200 GeV. In figure 2 (top-center) we observe that the other hadronic analyses also disfavor the low-mass region, though to a lesser degree, and two of these analyses (the H_{T}+$E_{\mathrm{T}}^{\mathrm{miss}}$+b-jets and the hadronic third generation) also exhibit secondary preferred regions around 1100 GeV, while figure 2 (top-right) shows that the EW, OS dilepton, and LS dilepton searches have little impact on the gluino mass distribution. Figure 2 (bottom-left) compares the prior distribution to posterior distributions after inclusion of the combined 7 TeV and combined 7+8 TeV data. The 7 TeV data already have sufficient sensitivity to exclude much of the low-mass gluino model space, and the 8 TeV data further strengthen this result.

The enhancements induced by the hadronic searches in the 800–1300 GeV range disappear in the combination since the observed excesses driving the enhancements are not consistent with a single model point or group of model points.

Figure 2 (bottom-center) shows the survival probability (eq. (4.1)) as a function of gluino mass for the combined 7 TeV, and 7+8 TeV results. The CMS searches exclude all the pMSSM points with a gluino mass below 500 GeV, and can probe scenarios up to the highest masses covered in the scan. While the direct production of gluinos with masses of order 3 TeV is beyond the reach of these searches, such gluinos are probed indirectly due

JHEP10(2016)129

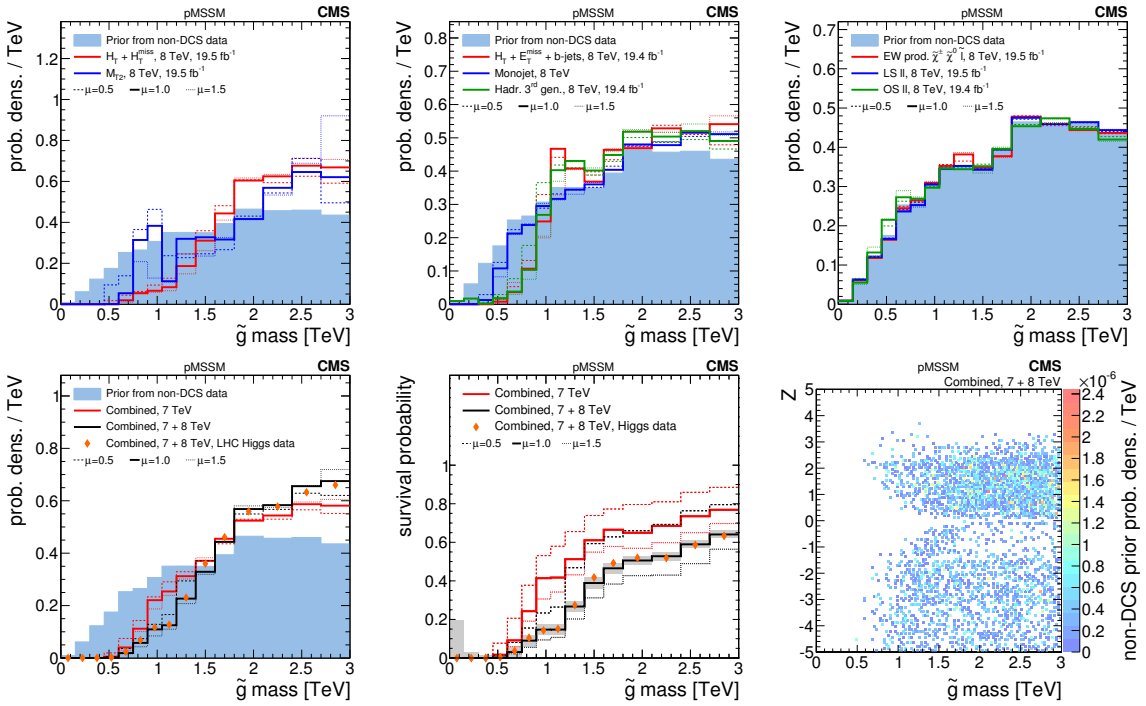

Figure 2. A summary of the impact of CMS searches on the probability density of the gluino mass in the pMSSM parameter space. The first-row and bottom-left plots compare the non-DCS prior distribution of the gluino mass (blue filled histograms) to posterior distributions after data from various CMS searches (line histograms), where the bottom-left plot shows the combined effect of CMS searches and the Higgs boson results. The bottom-center plot shows survival probabilities as a function of the gluino mass for various combinations of CMS data and data from Higgs boson measurements, where the shaded grey band gives the statistical uncertainty on the black histogram. The bottom-right plot shows the distribution of the gluino mass versus the Z-significance calculated from the combination of all searches.

the production of other lighter sparticles. In some cases, the production of lighter sparticles is enhanced by the presence of heavy gluinos, such as in the case of t-channel squark pair production.

Finally, figure 2 (bottom-left) shows the Z-significance versus gluino mass. A slight negative correlation for positive Z values and gluino masses is observed below 1200 GeV; Z declines slightly as mass increases, which indicates that some small excesses of events observed by the various searches are consistent with models with light gluinos.

Figures 3 and 4 similarly summarize the impact of searches on the first- and second-generation left-handed up squark mass and the mass of the lightest colored SUSY particle (LCSP), respectively. The picture is similar to that for the gluino mass. For both $\tilde{u}_L$ and the LCSP, the M_{T2} search shows a preference for masses from 500 to 1100 GeV. The overall impact of the searches on $\tilde{u}_L$ is less than the impact on the gluino mass owing to the more diverse gluino decay structure that can be accessed by a greater number of searches. For the LCSP, the overall impact is the least because the LCSP has the fewest decay channels; nevertheless, CMS searches exclude about 98% of the approximately 3000 model points

JHEP10(2016)129

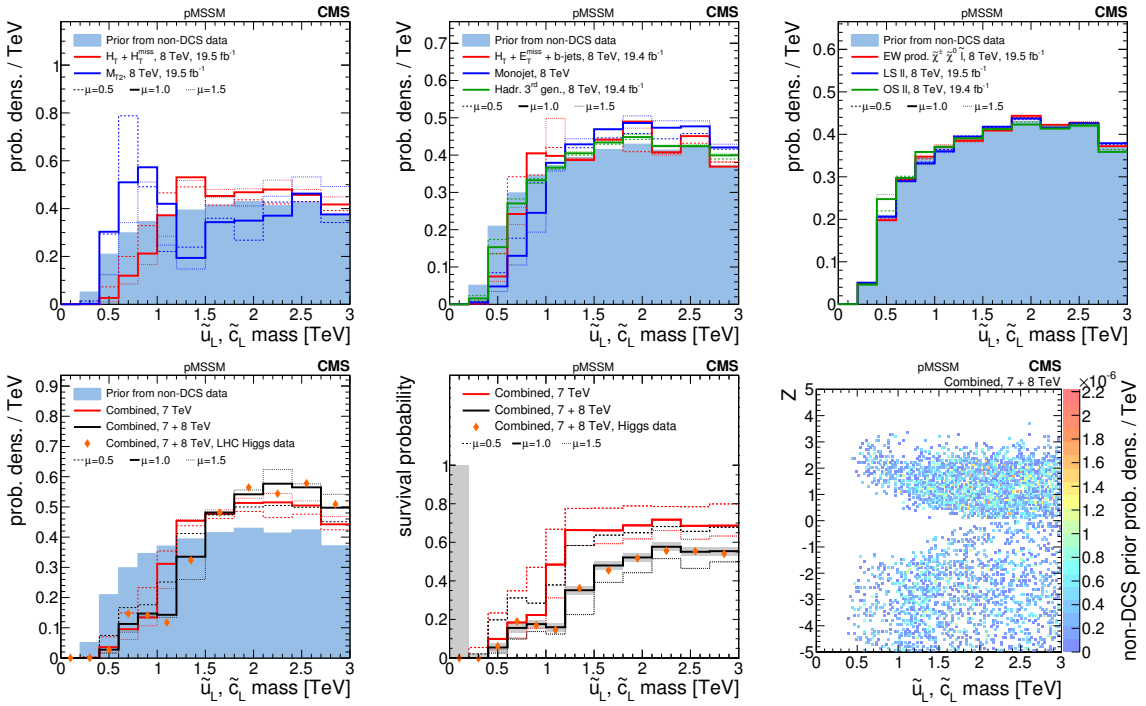

Figure 3. A summary of the impact of CMS searches on the probability density of the $\tilde{u}_L$ mass (equivalently, the $\tilde{c}_L$ mass) in the pMSSM parameter space. The first-row and bottom-left plots compare the non-DCS prior distribution of the $\tilde{u}_L$ mass to posterior distributions after data from various CMS searches, where the bottom-left plot shows the combined effect of CMS searches and the Higgs boson results. The bottom-center plot shows survival probabilities as a function of the $\tilde{u}_L$ mass for various combinations of CMS data and data from Higgs boson measurements. The bottom-right plot shows the distribution of the $\tilde{u}_L$ mass versus the Z-significance calculated from the combination of all searches. See figure 2 for a description of the shading.

with an LCSP mass below 300 GeV; in the surviving 2% of these model points, the LCSP is the $\tilde{D}_R$. We also see that the searches can be sensitive to scenarios with LCSP masses up to ∼1500 GeV. Again we find that the Higgs boson results make a negligible contribution. In each case we find a negative correlation between the Z-significance and the sparticle mass for positive Z values and masses below 1200 GeV; this is most pronounced for the LCSP.

Figure 5 illustrates what information this set of searches provides about the mass of the lightest top squark $\tilde{t}_1$. The difference between the prior and posterior distributions is minor. The reason is that the low-energy measurements like the $b \to s\,\gamma$ branching fraction (see table 1) impose much stronger constraints on the mass of the $\tilde{t}_1$ than do the considered analyses. This is not to say the CMS analyses are insensitive to top squark masses. The posterior distribution for the M_{T2} search exhibits an enhancement at $m_{\tilde{t}_1} < 1$ TeV relative to the non-DCS distribution. This enhancement does not appear in the combined posterior density because is suppressed by observations of other more sensitive searches. In the distribution of $m_{\tilde{t}_1}$ versus Z, the positive (negative) Z values have a slight negative (positive) correlation with the $\tilde{t}_1$ mass below 1 TeV, indicating that the CMS analyses considered have some direct sensitivity to top squarks with masses up to 1 TeV. The overall conclusion is that light top squarks with masses of the order of 500 GeV cannot be excluded.

JHEP10(2016)129

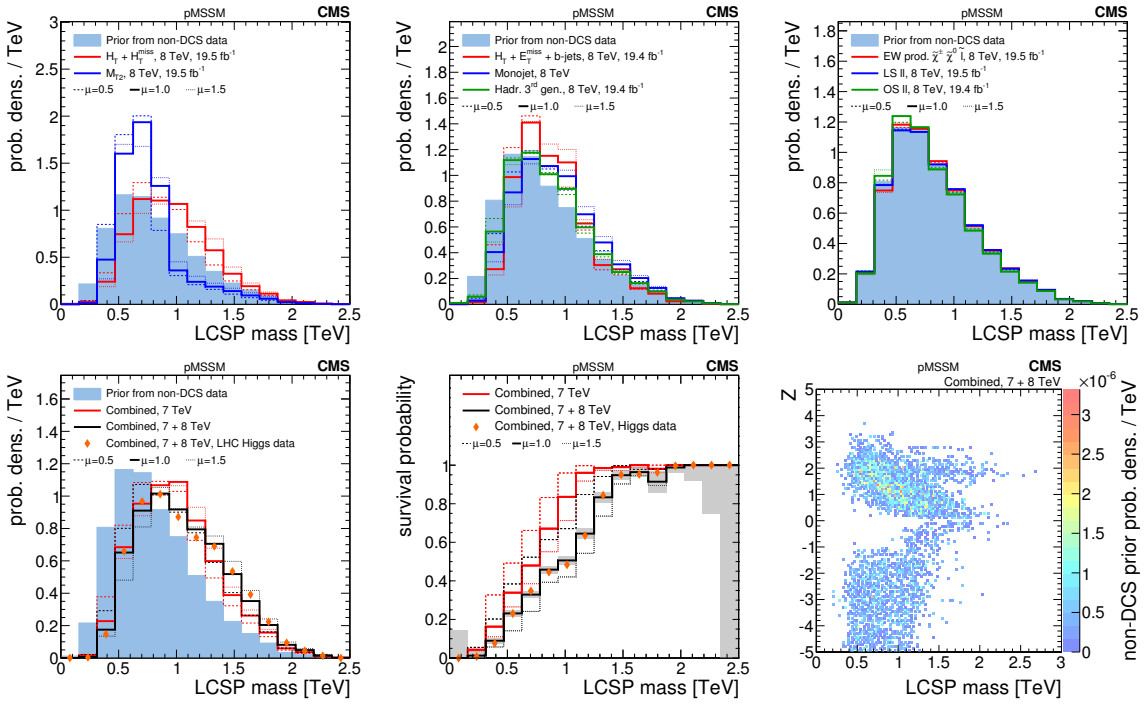

Figure 4. A summary of the impact of CMS searches on the probability density of the mass of the lightest colored SUSY particle (LCSP) in the pMSSM parameter space. The first-row and bottom-left plots compare the non-DCS prior distribution of the LCSP mass to posterior distributions after data from various CMS searches, where the bottom-left plot shows the combined effect of CMS searches and the Higgs boson results. The bottom-center plot shows survival probabilities as a function of the LCSP mass for various combinations of CMS data and data from Higgs boson measurements. The bottom-right plot shows the distribution of the LCSP mass versus the Z-significance calculated from the combination of all searches. See figure 2 for a description of the shading.

Turning now to the EW sector, we first show, in figure 6, the effect of the considered searches on our knowledge of the mass of the lightest neutralino $\widetilde{\chi}^0$. We see that the hadronic inclusive searches disfavor low $\widetilde{\chi}^0$ masses; the hadronic searches targeting specific topologies also have an effect, although smaller, and the leptonic searches have a marginal impact. The 7+8 TeV combined distribution is very similar to the M_{T2} distribution, especially in the lower mass region, indicating that this search is the most sensitive to the $\widetilde{\chi}^0$ mass. The main constraint on the $\widetilde{\chi}^0$ mass arises indirectly through correlations with other sparticle masses. Since $\widetilde{\chi}^0$ is the LSP, its mass is constrained by the masses of the heavier sparticles. As CMS searches push the probability distributions for the colored particles to higher values, more phase space opens for $\widetilde{\chi}^0$ and the $\widetilde{\chi}^0$ distributions shift to higher values. The survival probability distribution shows that no $\widetilde{\chi}^0$ mass is totally excluded at the 95% CL by CMS. In general, the nonexcluded points with light $\widetilde{\chi}^0$ are those with heavy colored sparticles. The fact that the survival probability decreases below a $\widetilde{\chi}^0$ mass of ∼700 GeV shows that CMS searches are sensitive up to this mass value. The Higgs boson data disfavor neutralino masses below about 60 GeV, that is, the mass range in which invisible decays $h \to \widetilde{\chi}^0_1\widetilde{\chi}^0_1$ could occur; this is visible in the first bin in figure 6 (bottom-left) (see ref. [51]).

JHEP10(2016)129

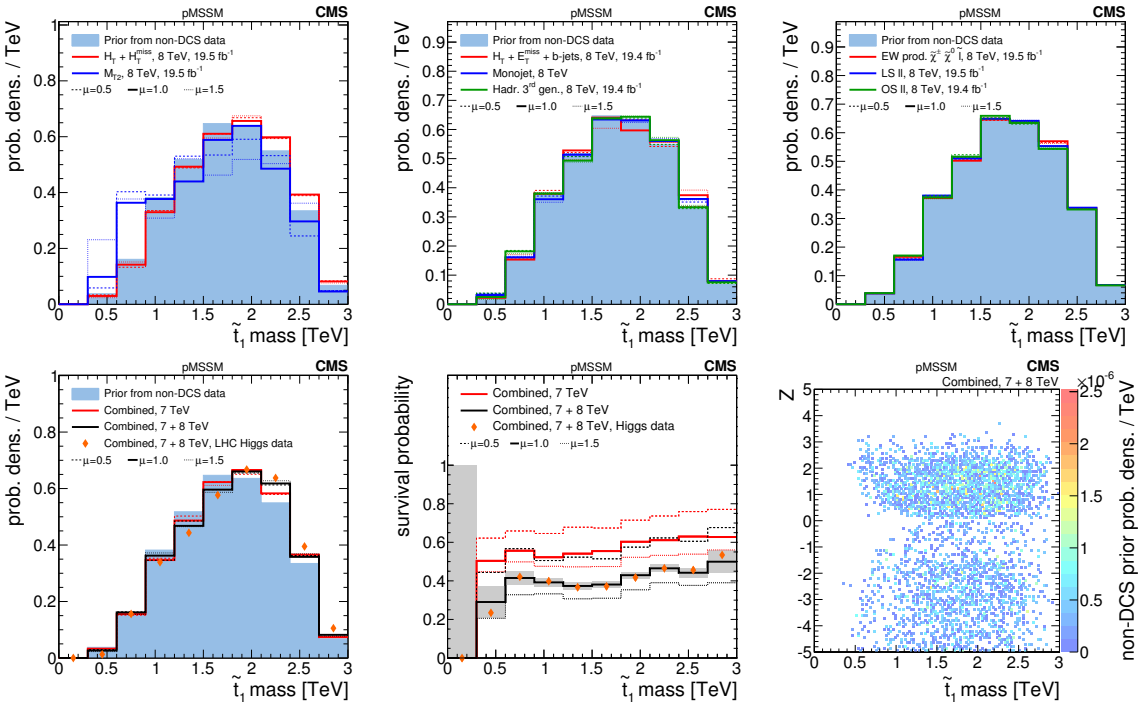

Figure 5. A summary of the impact of CMS searches on the probability density of the $\widetilde{t}_1$ mass in the pMSSM parameter space. The first-row and bottom-left plots compare the non-DCS prior distribution of the $\widetilde{t}_1$ mass to posterior distributions after data from various CMS searches, where the bottom-left plot shows the combined effect of CMS searches and the Higgs boson results. The bottom-center plot shows survival probabilities as a function of the $\widetilde{t}_1$ mass for various combinations of CMS data and data from Higgs boson measurements. The bottom-right plot shows the distribution of the $\widetilde{t}_1$ mass versus the Z-significance calculated from the combination of all searches. See figure 2 for a description of the shading.

In the MSSM, the lightest chargino becomes degenerate with the lightest neutralino for the condition $|M_1| \geq \min(|M_2|, |\mu|)$. Therefore, we define the lightest non-degenerate (LND) chargino as

$$\text{LND } \chi^{\pm} = \begin{cases} \widetilde{\chi}_1^{\pm} & \text{if} \quad |M_1| < \min(|M_2|, |\mu|) \\ \widetilde{\chi}_2^{\pm} & \text{if} \quad |M_1| > \min(|M_2|, |\mu|). \end{cases} \tag{4.2}$$

Figure 7 summarizes what information has been gained about the mass of the LND chargino. Again, the impact of the CMS searches is found to be rather limited and no chargino mass can be reliably excluded. It is worth noticing the impact of the leptonic searches. In figure 7 (top-right), the distributions differ from the non-DCS distribution, while these searches have negligible impact on most of the other SUSY observables and parameters considered in this study. We also note that the survival probability is lowest in the first bin where the LND $\widetilde{\chi}^{\pm}$ mass is between 0 and 200 GeV, but a small percentage of points still survive.

A more generic view is possible by looking at the overall CMS impact on the inclusive SUSY production cross section for 8 TeV, which is shown in figure 8. The most probable

JHEP10(2016)129

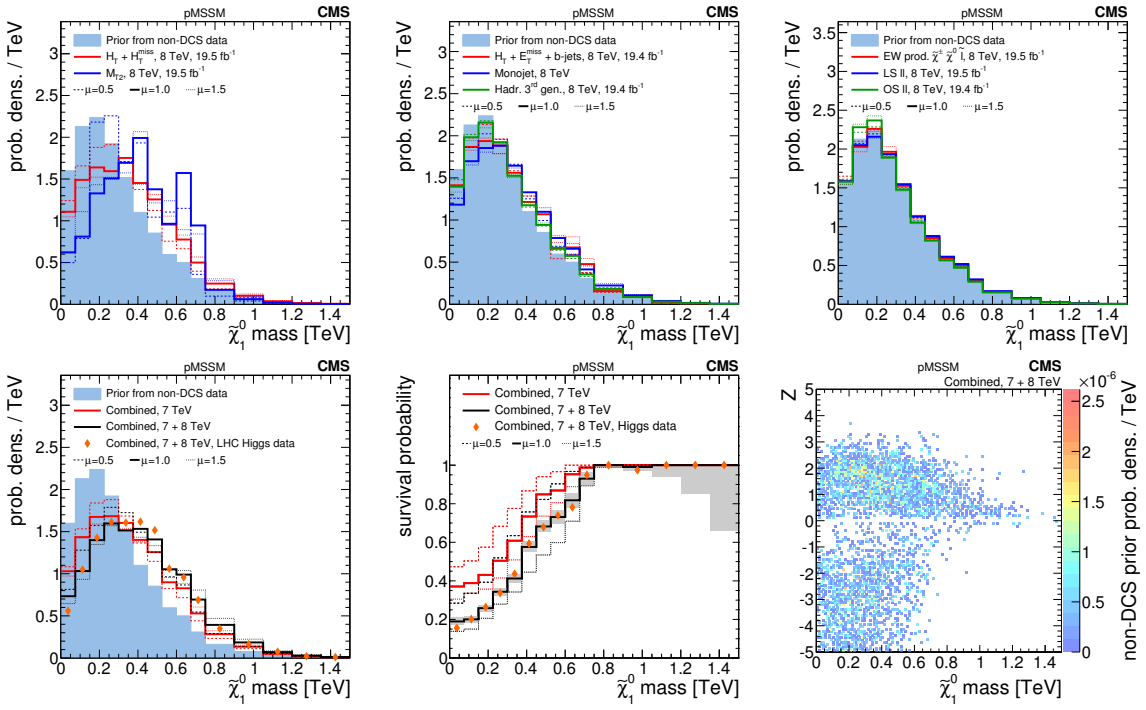

Figure 6. A summary of the impact of CMS searches on the probability density of the $\widetilde{\chi}_1^0$ mass in the pMSSM parameter space. The first-row and bottom-left plots compare the non-DCS prior distribution of the $\widetilde{\chi}_1^0$ mass to posterior distributions after data from various CMS searches, where the bottom-left plot shows the combined effect of CMS searches and the Higgs boson results. The bottom-center plot shows survival probabilities as a function of the $\widetilde{\chi}_1^0$ mass for various combinations of CMS data and data from Higgs boson measurements. The bottom-right plot shows the distribution of the $\widetilde{\chi}_1^0$ mass versus the Z-significance calculated from the combination of all searches. See figure 2 for a description of the shading.

total sparticle cross section in non-DCS prior is approximately 100 fb; the low tail of this distribution is shaped by the upper limits on the masses of sparticles in the prior. The effect of the CMS SUSY searches is to reduce this value by an order of magnitude. The inclusive H_{T}+$H_{\mathrm{T}}^{\mathrm{miss}}$ search has the largest individual contribution to this because of its ability to address a great diversity of final states comprising different sparticle compositions. The survival probability distribution confirms that CMS is sensitive to SUSY scenarios with total cross sections as low as 1 fb.

In figure 9, the non-DCS and post-CMS distributions are compared after 7 and 7+8 TeV data for several other important observables. We first note that the impact of the CMS data on the first and second generation right-handed up squarks is lower than on the corresponding left-handed up squarks (figure 3). This is because left-handed up squarks in the MSSM form doublets with mass-degenerate left-handed down squarks, while the right-handed up and down squarks are singlets and their masses are unrelated. Therefore, for the left-handed up squarks, the CMS sensitivity for a given mass is increased by the left-handed down squarks, which have the same mass. We also observe a mild impact on the bottom squark mass, where CMS disfavors masses below 400 GeV. The CMS searches also have

JHEP10(2016)129

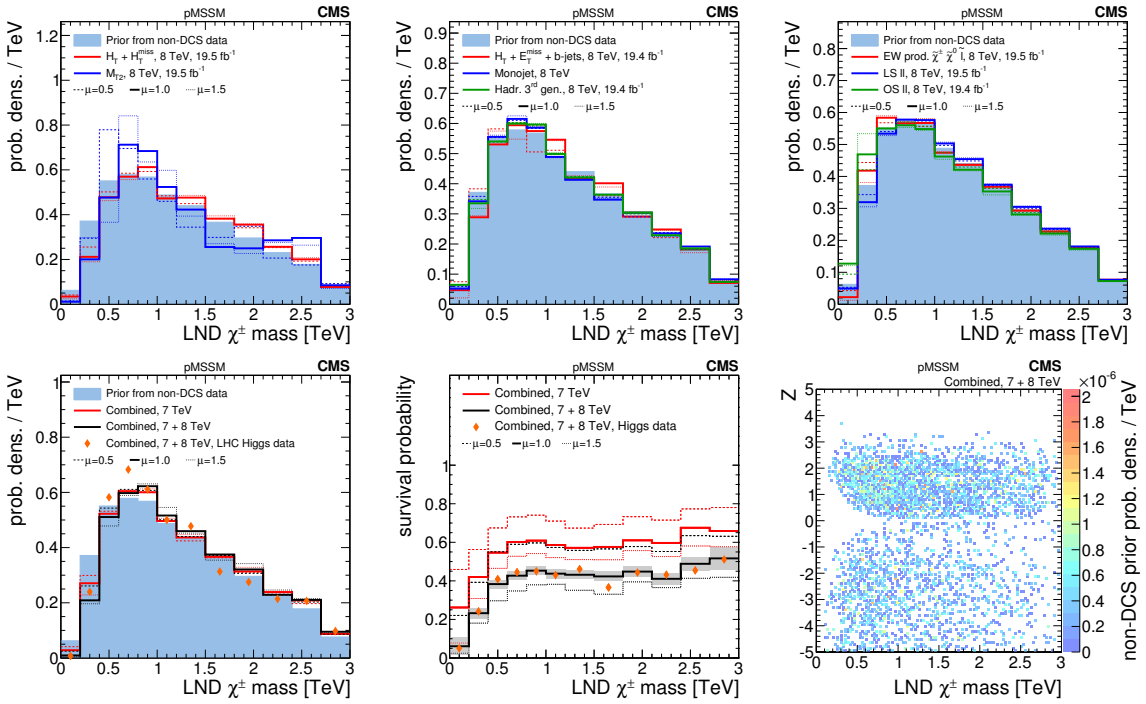

Figure 7. A summary of the impact of CMS searches on the probability density of the mass of the lightest non-degenerate (LND) chargino in the pMSSM parameter space. The first-row and bottom-left plots compare the non-DCS prior distribution of the LND $\widetilde{\chi}^{\pm}$ mass to posterior distributions after data from various CMS searches, where the bottom-left plot shows the combined effect of CMS searches and the Higgs boson results. The bottom-center plot shows survival probabilities as a function of the LND $\widetilde{\chi}^{\pm}$ mass for various combinations of CMS data and data from Higgs boson measurements. The bottom-right plot shows the distribution of the LND $\widetilde{\chi}^{\pm}$ mass versus the Z-significance calculated from the combination of all searches. See figure 2 for a description of the shading.

some sensitivity to the selectron and stau masses, which comes from the leptonic searches. The impact on $\widetilde{\chi}^{0}_{i\,2}$ and $\widetilde{\chi}^{\pm}$ masses is larger, mostly due to the dedicated EW analyses. The CMS SUSY searches have no impact on the masses of the light and heavy pseudoscalar Higgs bosons. The preference of the Higgs data for negative values of the higgsino mass parameter μ comes primarily from the fact that the measured signal strength normalized to its SM value for $Vh \to b\bar{b}$ (where V is a W or a Z boson) is currently slightly below one. In a SUSY model, this requires that radiative corrections reduce the bottom Yukawa coupling, thereby creating a preference for $\mu < 0$ [63]. The $\tan\beta$ distribution is largely unaffected by both the CMS SUSY searches and the current Higgs boson data evaluated via Lilith 1.01.

We also investigate the impact of the considered searches on some observables related to dark matter. Figure 10 shows distributions of the dark matter relic density, the spin-dependent (SD) direct detection cross section, and spin-independent (SI) direct detection cross section. In figure 10 (left), the relic density is seen to take on a bimodal probability density. The lower peak corresponds primarily to model points with bino-like LSPs, and the upper peak is mainly due to points with wino- and higgsino-like LSPs. The combined CMS searches lead to a noticeable enhancement of the lower peak. In figure 10 (center)

JHEP10(2016)129

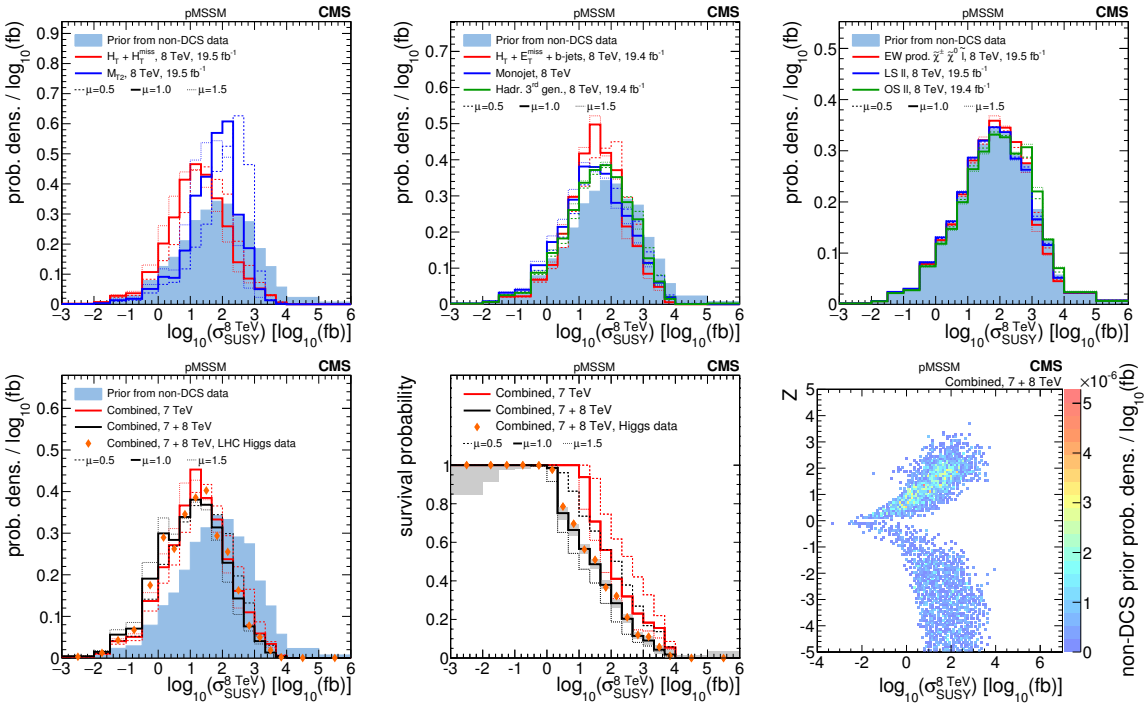

Figure 8. A summary of the impact of CMS searches on the probability density of the logarithm of the cross section for inclusive sparticle production in 8 TeV pp collisions, $\log_{10}(\sigma^{8\,\mathrm{TeV}}_{\mathrm{SUSY}})$, in the pMSSM parameter space. The first-row and bottom-left plots compare the non-DCS prior distribution of the $\log_{10}(\sigma^{8\,\mathrm{TeV}}_{\mathrm{SUSY}})$ to posterior distributions after data from various CMS searches, where the bottom-left plot shows the combined effect of CMS searches and the Higgs boson results. The bottom-center plot shows survival probabilities as a function of the $\log_{10}(\sigma^{8\,\mathrm{TeV}}_{\mathrm{SUSY}})$ for various combinations of CMS data and data from Higgs boson measurements. The bottom-right plot shows the distribution of the $\log_{10}(\sigma^{8\,\mathrm{TeV}}_{\mathrm{SUSY}})$ versus the Z-significance calculated from the combination of all searches. See figure 2 for a description of the shading. In plot (bottom left), the apparent enhancement of the left tail of the posterior density with respect to the prior is due to the suppression of the right tail and an overall renormalization.

and (right), minor differences are seen between the prior and posterior densities for the direct detection cross section.

4.3 Correlations among pMSSM parameters

A virtue of high-dimensional models like the pMSSM is that they enable the examination of correlations among parameters not possible in the context of more constrained models.

Figure 11 compares marginalized distributions in two dimensions of non-DCS (left) to post-CMS distributions (middle), and also shows the post-CMS to non-DCS survival probability (right) for several observable pairs. The first two rows of distributions show that the CMS impact on our knowledge of the $\widetilde{\chi}^0$ mass is strongly correlated with the gluino or the LCSP mass. Since $\widetilde{\chi}^0$ is the LSP, light colored particles imply a light $\widetilde{\chi}^0$. Consequently, the disfavoring of light colored sparticles implies the disfavoring of a light $\widetilde{\chi}^0$. In the last row, it is seen that the $\widetilde{\chi}^0$ mass is correlated most strongly with the cross section

JHEP10(2016)129

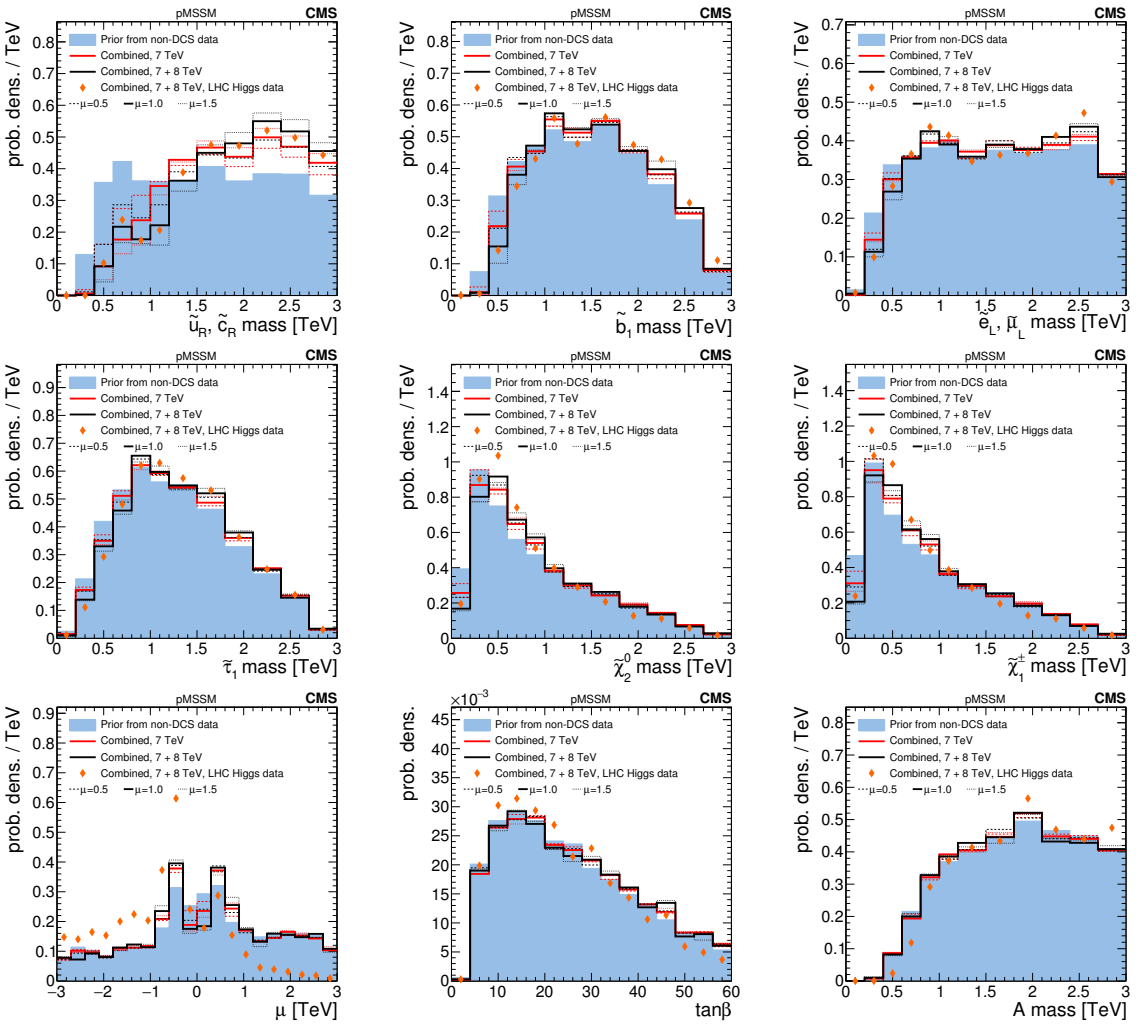

Figure 9. Comparison of prior and posterior distributions after several combinations of data from the CMS searches for the $\widetilde{u}_R, \widetilde{c}_R$ mass, $\widetilde{b}_1$ mass, $\widetilde{e}_L, \widetilde{\mu}_L$ mass, $\widetilde{\tau}_1$ mass, $\widetilde{\chi}^0_2$ mass, $\widetilde{\chi}^\pm$ mass, the higgsino mass parameter μ, $\tan\beta$, and A mass.

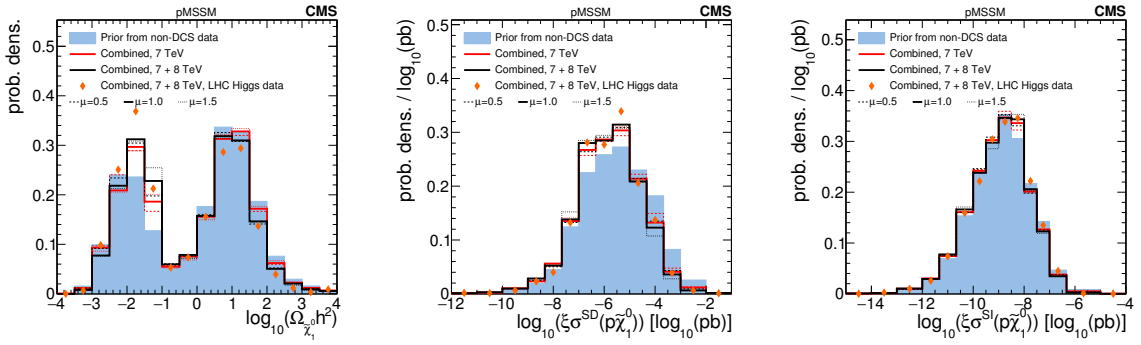

Figure 10. Comparison of prior and posterior distributions after several combinations of data from the CMS searches for $\Omega_{\widetilde{\chi}^0_1}$, $\xi\sigma^{\mathrm{SD}}(p\widetilde{\chi}^0_1)$, and $\xi\sigma^{\mathrm{SI}}(p\widetilde{\chi}^0_1)$.

JHEP10(2016)129

and that light $\widetilde{\chi}^0$ LSPs are indeed disfavored for the reason just given. We note, however, that scenarios with $\widetilde{\chi}^0$ masses around 100 GeV can still survive even though they have cross sections above 1 pb. These and other high cross section model points are discussed in section 5. In the third row, we show the probability distributions and survival probability for $\widetilde{\chi}^0$ versus $\widetilde{\mathrm{t}}_1$ mass. Here we see that, although the post-CMS probabilities shift towards higher values, the survival probabilities never really go down to zero. Although current SMS scenarios exclude large parts of the $\widetilde{\mathrm{t}}_1$-$\widetilde{\chi}^0$ plane, we see that pMSSM scenarios with relatively low $\widetilde{\mathrm{t}}_1$ masses (500 GeV) are not significantly disfavored by the CMS searches considered. We note that the searches for top squark production considered here focus primarily on the decay channel $\tilde{\mathrm{t}}_1 \to \mathrm{t}\widetilde{\chi}^0_1$, and it may be that a greater impact would be observed if the searches targeting leptonic channels were incorporated in this study.

Studies were performed to assess how the conclusions would change if a different choice of initial prior had been made. A log-uniform prior ($p_0(\theta)$ in eq. (3.3)) is found to yield posterior densities very similar to those from the nominal uniform prior. The most significant exception is that the densities for the masses of the $\widetilde{\chi}^0$ and $\widetilde{\chi}^{\pm}$ are shifted 10–20% toward higher values with respect to the densities derived from the uniform prior. It is found that the marginalized likelihood distributions are consistent with the profile likelihoods, suggesting that a frequentist analysis based on the profile likelihoods would yield similar conclusions.

5 Nonexcluded regions in the pMSSM parameter space

Of the 7200 pMSSM points considered in this study, about 3700 cannot be excluded by CMS analyses based on their Z-significance (figure 1 (bottom right)), although more than half of these nonexcluded points have a total cross section greater than 10 fb at $\sqrt{s} = 8$ TeV. It is of interest to characterize this nonexcluded subspace in order to shed light on why the CMS analyses are not sensitive to these points, which can help guide the design of future analyses. To this end, we decompose the nonexcluded subspace into the dominant physical processes and follow with an idealized analysis of final state observables.

For the decomposition, signal events are analyzed at the generator level for each model point, and the pair of SUSY particles most frequently produced directly from the proton-proton interaction is taken as the production mode for that model point. Then the principal (dominant) process for that point is built as a tree diagram starting from the pair of SUSY mother particles and following the decay modes with the highest branching fractions until endpoints consisting of only SM particles and LSPs are reached. Indices of particle charge, flavor, and chirality are ignored in the construction, with the exception of the flavor of the third-generation squarks and quarks. Over 100 distinct principal processes are found among the total 7200 studied points, of which the first twelve are listed in figure 12. Many of the principal processes are seen to correspond to common SMS scenarios, while others depict more unusual scenarios with long decay chains.

The distribution of principal processes for excluded and nonexcluded points is given in figure 13 (left). It is seen that processes involving direct gluino production (5 and 8) are excluded with a much higher frequency than they survive, and those with EW gaug-

JHEP10(2016)129

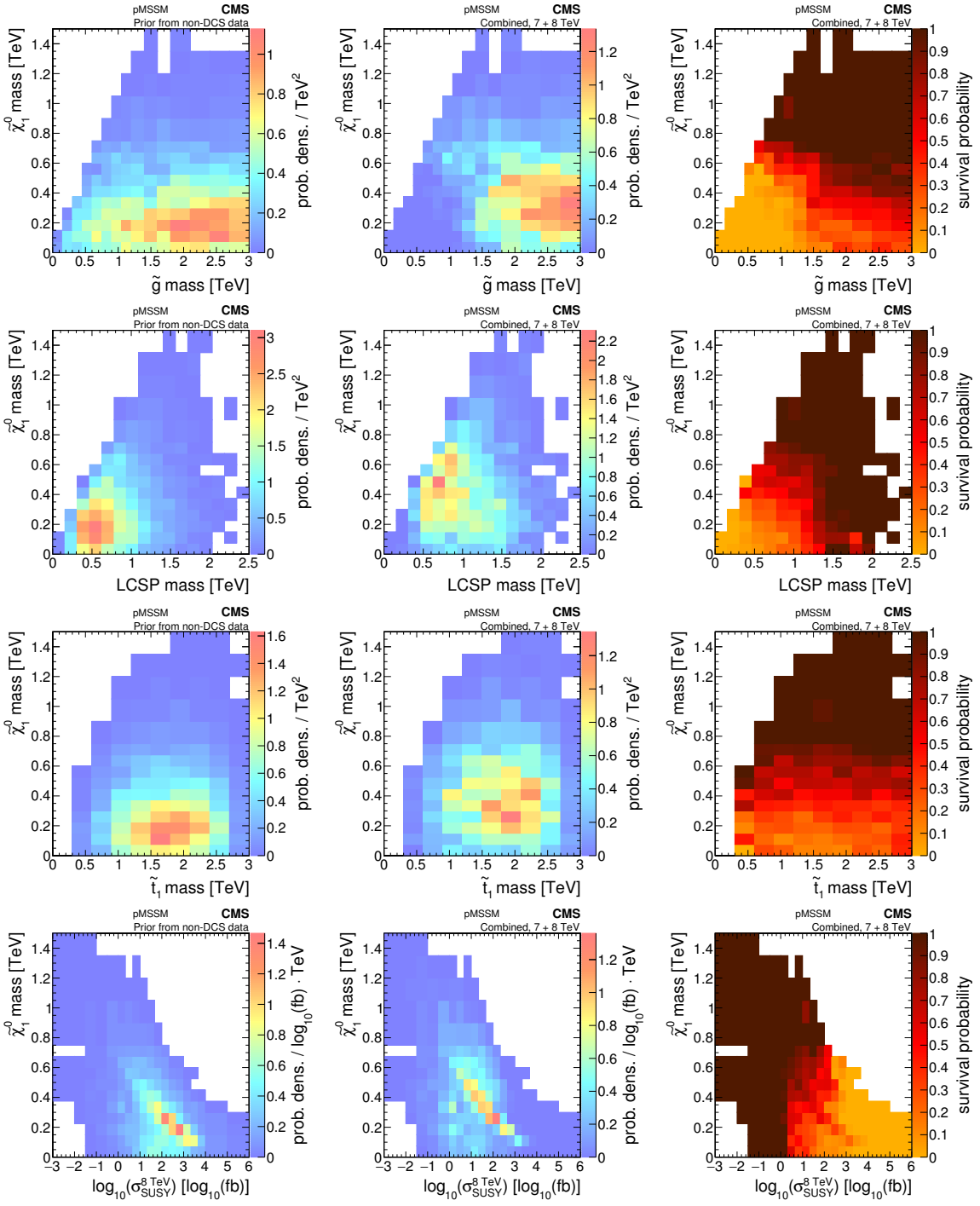

Figure 11. Marginalized non-DCS distributions (first column), compared with posterior distributions (second column) and survival probabilities (third column) after inclusion of the considered CMS searches, are shown for the $\tilde{\chi}_1^0$ mass versus gluino mass (first row), the LCSP mass (second row), the top squark mass (third row), and the logarithm of the cross section for inclusive sparticle production at 8 TeV (bottom row).

JHEP10(2016)129

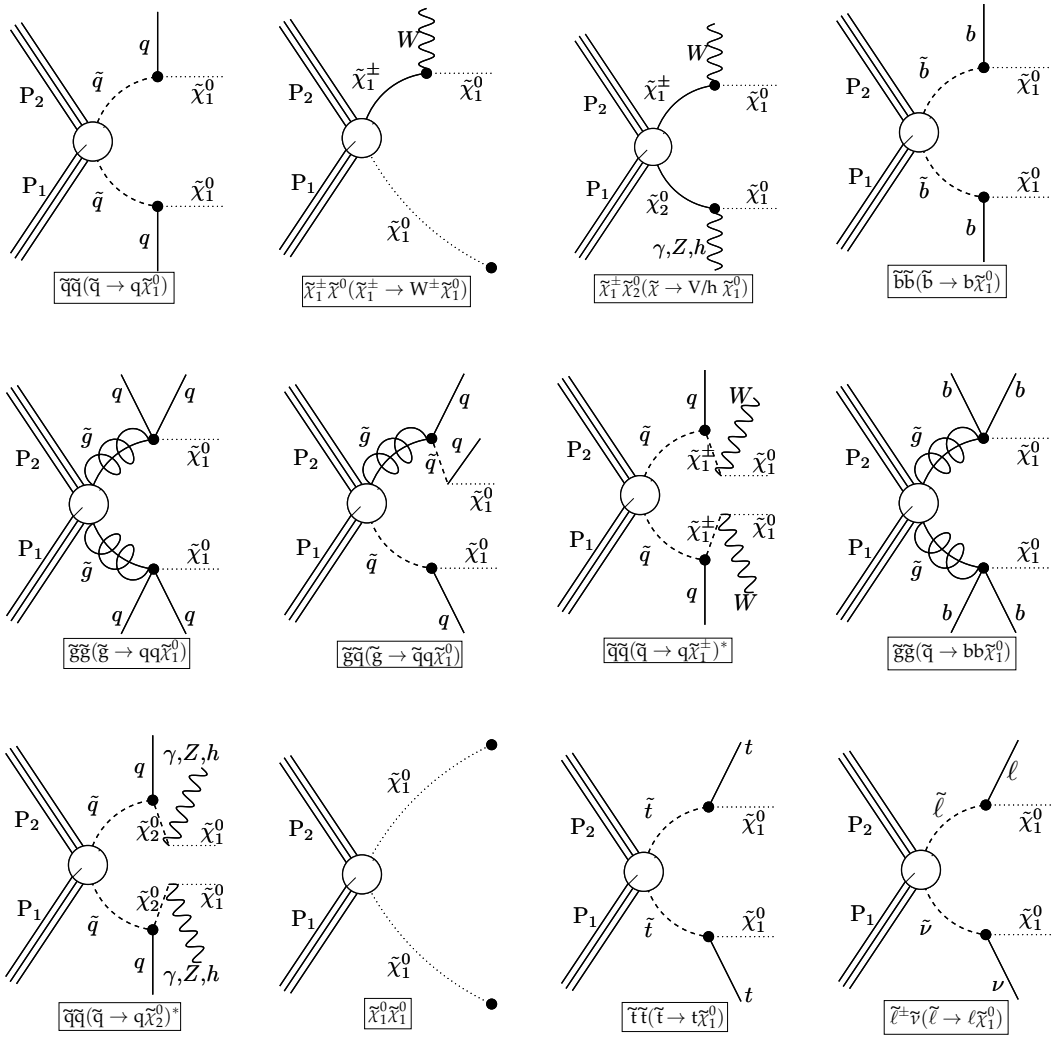

Figure 12. The twelve most common principal processes in the pMSSM, listed in order of their frequency before the constraints of the CMS searches. Both on-shell and off-shell states are included. Indices of particle charge, flavor, and chirality are ignored in the construction, with the exception of the flavor of the third-generation squarks and quarks. Asterisks in the labels indicate where process names involving long decay chains have been abbreviated.

ino production (2, 3, and 10) survive with a higher frequency than they are excluded. Processes with first-generation squark production (1 and 7) survive and are excluded at similar rates, and processes with slepton production (12) have exceptionally high survival rates. These trends are likely attributable to the difference in the production cross section between colored and noncolored particles for a given SUSY mass scale. The overflow bin (other), which contains many principal processes, including modes of colored and noncolored particle production, indicates a survival rate approximately equal to the exclusion rate. The dominance is defined for each model point as the ratio of the cross section of the principal process to the total SUSY production cross section at 8 TeV,

$$\text{dominance} \equiv \sigma^{8\,\text{TeV}}_{\text{principal}}/\sigma^{8\,\text{TeV}}_{\text{tot}}, \tag{5.1}$$

JHEP10(2016)129

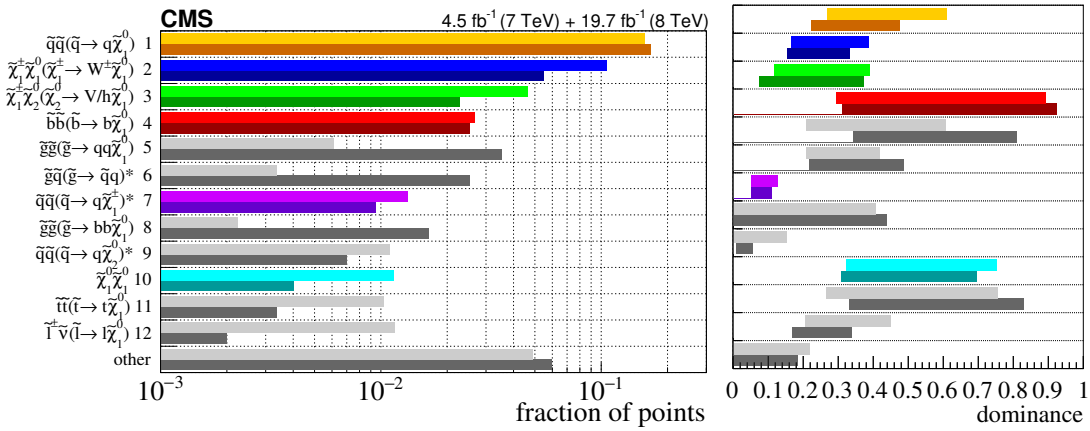

Figure 13. The left plot shows the fraction of excluded (dark) and nonexcluded (light) points out of all considered points, by principal process. Color is assigned to the processes that are most common after the constraints of the CMS searches, which are selected for further study. The dominance of principal processes, as defined in eq. (5.1), is given in the right plot, where the bands show the RMS range of the dominance.

and is shown in figure 13 (right). Most values of the dominance are in the range 0.05–0.60. The excluded and nonexcluded values for the dominance are seen to agree within the RMS of the distributions, indicating that the presence of multiple event signatures within a single model hypothesis does not significantly impact our ability to exclude such a model point.

Dedicated searches exist that correspond to some of the most frequent principal processes, indicating areas where the SMS approach is likely well optimized. For example, points with principal processes 1, $\tilde{q}\tilde{q}(\tilde{q}\to q\tilde{\chi}_1^0)$, and 4, $\tilde{b}\tilde{b}(\tilde{b}\to b\tilde{\chi}_1^0)$, enjoy searches that target these processes explicitly. A few principal processes have not been explicitly targeted by the host of CMS SUSY searches, including processes 2, $\tilde{\chi}_1^\pm\tilde{\chi}^0(\tilde{\chi}_1^\pm\to W^\pm\tilde{\chi}_1^0)$, and 3, $\tilde{\chi}_1^\pm\tilde{\chi}_2^0(\tilde{\chi}\to V/h\tilde{\chi}_1^0)$, the asymmetric EW gaugino production modes. New searches that target these or the other processes with insufficient coverage may serve to broaden the overall sensitivity to the pMSSM.

Next, we characterize the nonexcluded model space by the predicted final states to shed light on what signatures may serve to target the nonexcluded points in Run 2. We define a set of loose baseline physics objects and event variables, at the generator level, as follows:

- Leptons: electrons, muons, or taus having a transverse momentum p_T greater than 5 GeV and an isolation less than 0.2. Here, isolation $= [(\Sigma_i p_{T\,i}) - p_T]/\Sigma_i p_{T\,i}$, where the sums run over all detector-visible particles i within a ΔR cone of 0.5 around the object, with $\Delta R = \sqrt{(\Delta\eta)^2 + (\Delta\phi)^2}$, where η is the pseudorapidity and ϕ is the azimuthal angle in radians;

- Jets: particles clustered with the anti-k_T jet algorithm [69] with distance parameter 0.5. The jets are required to have a p_T greater than 20 GeV;

- b-jets: jets matched to a b hadron within a ΔR of 0.5;

JHEP10(2016)129

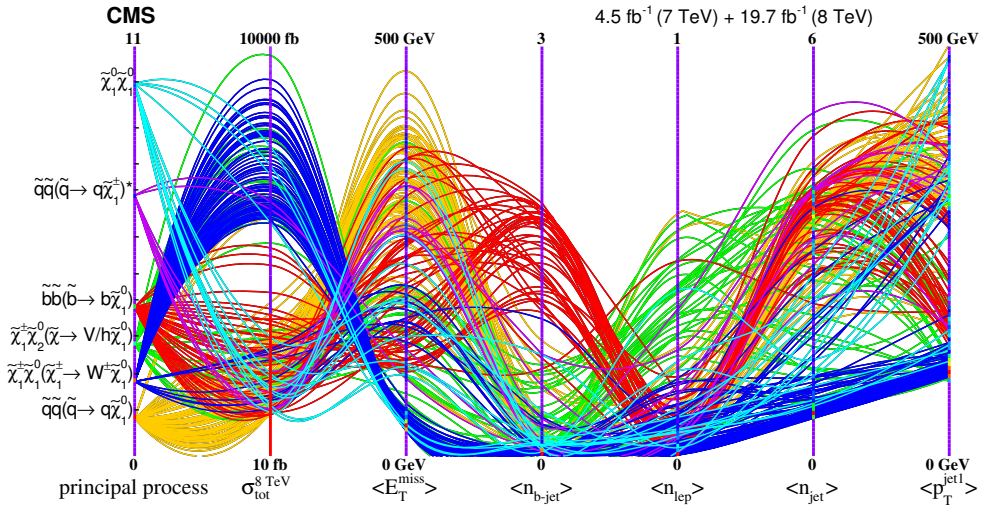

Figure 14. A parallel coordinates plot showing several hundred selected nonexcluded model points for the six most common principal processes, with seven key properties. From the left, the selected properties are: the principal process, the 8 TeV signal production cross section (in $\log_{10}$ scale), the average value of the $E_{\mathrm{T}}^{\mathrm{miss}}$, the average number of b-jets, leptons, and jets, and finally, the average p_{T} momentum of the leading jet. Color is assigned based on the principal process. Orange codes for process 1, blue for process 2, green for 3, red for 4, violet for 7, and cyan for 10. The range of each axis is given at its lower and upper end. Lines arching toward higher vertical positions typically indicate more "discoverable" scenarios.

- $E_{\mathrm{T}}^{\mathrm{miss}}$: the missing transverse energy, calculated as the magnitude of the vector sum of the transverse momenta of visible particles with $p_{\mathrm{T}} > 5\,\mathrm{GeV}$;
- H_{T}: the scalar sum of the p_{T} of the jets with a $p_{\mathrm{T}} > 50\,\mathrm{GeV}$.

We use a parallel coordinates visualization technique that enables the display of multiple dimensions. In figure 14, we show nonexcluded points corresponding to the six selected principal processes (those denoted by color in figure 14). Vertical axes are chosen to represent meaningful properties of the model points, and each model point is represented as a curved line traversing the plot from left to right, intersecting each axis at the parameter value taken by the model point. The curvature of the lines is added to help distinguish between similar pMSSM points, but the trajectories of the lines between the axes do not carry physical information. A number of distinct scenarios are seen to have survived the CMS analyses. A minimum threshold of 20 fb has been applied to the 8 TeV signal cross sections to limit the scope to those points that could potentially still be probed with the Run 1 data set using an expanded set of analyses and techniques.

The nonexcluded points associated with principal processes 1, $\widetilde{\mathrm{qq}}(\widetilde{\mathrm{q}} \to \mathrm{q}\widetilde{\chi}_1^0)$, and 4, $\widetilde{\mathrm{bb}}(\widetilde{\mathrm{b}} \to \mathrm{b}\widetilde{\chi}_1^0)$, are seen to give rise to large average $E_{\mathrm{T}}^{\mathrm{miss}}$, jet multiplicities between 2 and 4, and moderate to low cross sections due the the large masses of the squarks. Given the higher cross sections in Run 2, these high $E_{\mathrm{T}}^{\mathrm{miss}}$ scenarios will become increasingly more accessible.

Model points with principal processes 2, $\widetilde{\chi}_1^{\pm}\widetilde{\chi}^0(\widetilde{\chi}_1^{\pm} \to \mathrm{W}^{\pm}\widetilde{\chi}_1^0)$, and 3, $\widetilde{\chi}_1^{\pm}\widetilde{\chi}_2^0(\widetilde{\chi} \to \mathrm{V/h}\widetilde{\chi}_1^0)$, typically predict large cross sections, in the range between 100 fb and 1 pb, but a

JHEP10(2016)129

limited number of physical observables with discriminating power, primarily due to compression in the mass spectrum between the LSP and the other EW gauginos. These points peak low in the average multiplicity of jets, leptons, and in average $E_{\mathrm{T}}^{\mathrm{miss}}$. They could potentially be probed with searches that involve events with initial state radiation and soft boson decay products that are aligned with the $E_{\mathrm{T}}^{\mathrm{miss}}$. We note that process 2 is the principal process that characterizes the pMSSM point with the largest Z-significance, 3.6. This model point corresponds to a $\widetilde{\chi}_1^0$ mass of around 200 GeV and a mass difference between the lightest chargino and LSP of about 3 GeV, which are properties of many model points that survived the CMS analyses.

Points with principal processes 3, $\widetilde{\chi}_1^{\pm}\widetilde{\chi}_2^0(\widetilde{\chi} \to \mathrm{V/h}\widetilde{\chi}_1^0)$, and 10, $\widetilde{\chi}_1^0\widetilde{\chi}_1^0$, tend to follow the trend profiled by process 2, $\widetilde{\chi}_1^{\pm}\widetilde{\chi}^0(\widetilde{\chi}_1^{\pm} \to \mathrm{W}^{\pm}\widetilde{\chi}_1^0)$, differing primarily in the lepton multiplicity and, in the case of at least one lepton, in the average p_{T} of the highest-p_{T} lepton (leading lepton). The close resemblance of processes 10 and 2 is mostly due to the fact that the mass difference between the $\widetilde{\chi}_1^{\pm}$ and $\widetilde{\chi}_1^0$ is frequently very small (less than 3 GeV), causing the ensuing off-shell W boson of process 2 to produce undetectably soft objects.

Points with principal processes 5, $\widetilde{\mathrm{g}}\widetilde{\mathrm{g}}(\widetilde{\mathrm{g}} \to \mathrm{qq}\widetilde{\chi}_1^0)$, and 6, $\widetilde{\mathrm{g}}\widetilde{\mathrm{q}}(\widetilde{\mathrm{g}} \to \widetilde{\mathrm{q}}\mathrm{q}\widetilde{\chi}_1^0)$, the most frequent modes involving gluinos, are not highlighted in figure 14, since their frequency among nonexcluded points is relatively small. We note that several of the nonexcluded models with very light gluino masses (less than 700 GeV) correspond to principal process 6, with mass differences between the $\widetilde{\mathrm{g}}$ and LSP that range around 100 GeV. Sensitivity to these model points may be possible by considering final states with three or fewer jets and $E_{\mathrm{T}}^{\mathrm{miss}}$ thresholds that are lower than typically applied.

Points with principal process 7, $\widetilde{\mathrm{q}}\widetilde{\mathrm{q}}(\widetilde{\mathrm{q}} \to \mathrm{q}\widetilde{\chi}_1^{\pm})^*$, do not display distinct trends in the properties selected, which is partly due to these points having a low dominance of around 0.1. Such model points have a diverse set of secondary processes, which are not directly examined here.

A general observation about the model points in figure 14 is the significant anticorrelation of observables, which manifests as the criss-crossing of lines between the axes. For example, model points with very high average $E_{\mathrm{T}}^{\mathrm{miss}}$ tend to have very low cross sections, and vice versa. This is a consequence of the fact that, no significant excess of events having been observed in data, the surviving model points are those with very few experimentally accessible observables; otherwise they would have been excluded.

We note that the surviving pMSSM point with the lowest value of $m_{\widetilde{\mathrm{g}}}$ (about 600 GeV) is not characterized by one of the twelve most frequent principle processes discussed above, but by processes involving gluino pair production, where each gluino decays into two light-flavor quarks and an EW gaugino, and where the EW gaugino subsequently decays into a vector boson and an LSP. The mass difference between the intermediate gaugino and the LSP is about 5 GeV, which, in most events, does not leave enough energy for the vector bosons to have decay products that are reconstructed in the detector.

With over 50% of all nonexcluded points corresponding to cross sections of greater than 10 fb, it is critical to further examine why these points were not accessed in Run 1. We attempt to gain an understanding by further characterizing the signal, evaluating fiducial cross sections corresponding to a range of final-state observables. The fiducial cross

JHEP10(2016)129

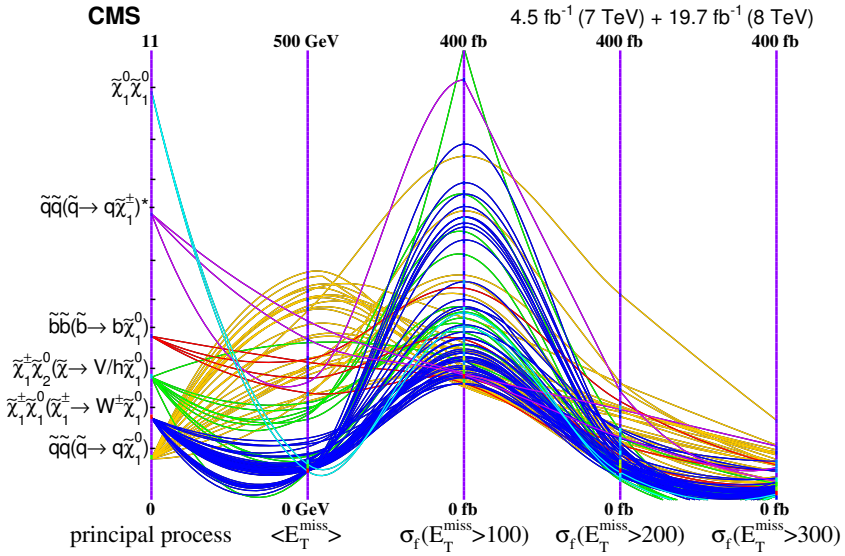

Figure 15. A parallel coordinates plot of the nonexcluded pMSSM points with the axes set as the principal process, the average $E_{\mathrm{T}}^{\mathrm{miss}}$ (in GeV), and the fiducial cross section (in linear scale) for various thresholds on the $E_{\mathrm{T}}^{\mathrm{miss}}$. All nonexcluded points corresponding to processes 1, 2, 3, 4, 7, and 10 that have a fiducial cross section for $E_{\mathrm{T}}^{\mathrm{miss}} > 100\,\mathrm{GeV}$ greater than 100 fb are shown. Color is assigned to values of the principal process in the same manner as in figure 14.

section σ_{f} of a final-state is defined for each model point as

$$\sigma_{\mathrm{f}} = \sigma_{\mathrm{tot}}^{8\,\mathrm{TeV}} A, \tag{5.2}$$

where A is the acceptance times signal efficiency computed as the fraction of simulated signal events passing a set of event-level criteria. We examine a set of final-state observables that loosely correspond to trigger thresholds or signal regions of the examined searches. Figures 15–17 show the impact of adjusting various thresholds on the fiducial cross sections of nonexcluded points.

Some principal processes can be associated with large fiducial cross sections, depending on the final state considered. For example, points with mostly first-generation squark production give rise to large fiducial cross sections for events with high H_{T}, resulting in figure 16 showing mostly orange-colored points; and points with production involving EW gauginos give rise to substantial fiducial cross sections for events with a high multiplicity of soft leptons, which explains the unaccompanied blue and green lines in figure 17. Somewhat striking is the behavior of the $E_{\mathrm{T}}^{\mathrm{miss}}$ fiducial cross section (figure 15), which can increase rapidly (by up to a factor of ten) as the threshold is relaxed from 200 to 100 GeV. It is apparent that many of the nonexcluded regions are not accessible with thresholds of 200 GeV, a common criterion applied offline to achieve full efficiency with the triggers. The fiducial cross section decreases noticeably as the threshold is further increased from 200 to 300 GeV. Similar behavior is seen for the H_{T} fiducial cross section (figure 16). Fiducial cross sections are quite large for these final states when a threshold of 300 GeV is applied, but fall off substantially for higher thresholds.

JHEP10(2016)129

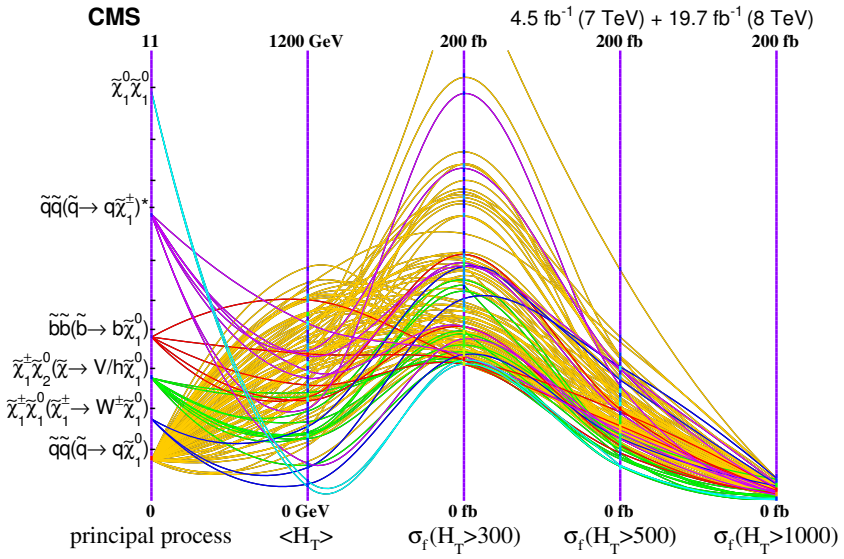

Figure 16. A parallel coordinates plot of the nonexcluded pMSSM points with the axes set as the principal process, the average H_{T} (in GeV), and the fiducial cross section (in linear scale) for various thresholds on the H_{T}. All nonexcluded points corresponding to processes 1, 2, 3, 4, 7, and 10 that have a fiducial cross section for $H_{\mathrm{T}} > 300\,\mathrm{GeV}$ greater than 300 fb are shown. Color is assigned to values of the principal process in the same manner as in figure 14.

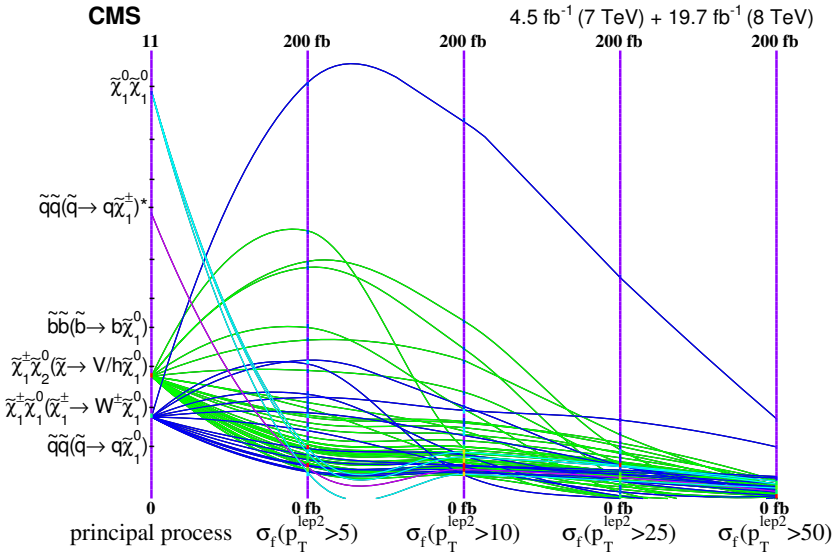

Figure 17. A parallel coordinates plot of the nonexcluded pMSSM points with the axes set as the principal process and the fiducial cross section (in linear scale) for various thresholds on the sub-leading lepton p_{T} (in GeV). All nonexcluded points corresponding to processes 1, 2, 3, 4, 7, and 10 that have a fiducial cross section for $p_{\mathrm{T}}^{\mathrm{lep2}} > 5\,\mathrm{GeV}$ greater than 30 fb are shown. Color is assigned to values of the principal process in the same manner as in figure 14.

JHEP10(2016)129

Of course, a loosening of the object thresholds would increase the background yield as well as signal yield. Thorough analysis of specific backgrounds will be necessary to select optimal values for kinematic thresholds and other analysis techniques to probe the most difficult points. However, the lesson that nonexcluded pMSSM models have large cross sections in background-rich kinematic regions is an open invitation for the development of new techniques that improve signal to background discrimination and background modeling.

6 Summary

The impact of a representative set of the 7 and 8 TeV CMS SUSY searches on a potentially accessible subspace of the minimal supersymmetric standard model (pMSSM) has been investigated. The subspace of the pMSSM is defined by restricting the ranges of the 19 pMSSM parameters to values that are either physically motivated or that correspond to models that are potentially accessible in the long-term LHC program. An additional restriction is imposed that the lightest chargino decay promptly or with a lifetime that leads to at most a short decay length in the detector. The set of searches, taken individually and in combination, include those with all-hadronic final states, like-sign and opposite-sign charged leptons, and multiple leptons in configurations sensitive to electroweak production of superpartner particles. They are found to exclude all analyzed pMSSM points with a gluino mass less than 500 GeV (approximately 250 of the 7200 sample points), and 98% of scenarios in which the lightest colored supersymmetric particle is less than 300 GeV. While the sensitivity of searches to top squarks extends up to $m_{\tilde{t}_1} \approx 700\,\text{GeV}$, the overall impact on the top squark mass is small because the region of highest sensitivity, $m_{\tilde{t}_1} \lesssim 500\,\text{GeV}$, is already suppressed by the results of previous experiments, such as the measurement of the $b \to s\gamma$ branching fraction. Neutralino and chargino masses less than 300 GeV are significantly disfavored, but not ruled out, by the CMS data. Measurements of the Higgs boson mass and signal strengths are included in this study, but add little to the model constraints.

Approximately half of this potentially-accessible subspace of the pMSSM is excluded by the CMS data. Of the surviving points, about half have cross sections greater than 10 fb, and some have cross sections greater than 1 pb. Most high cross section points correspond to electroweak gaugino production with mass splittings between the second-lightest and the lightest SUSY particle less than 3 GeV. Nonexcluded model points with low-mass gluinos correspond to processes involving intermediate electroweak gauginos that are nearly degenerate with the lightest SUSY particle. The surviving points evade the experimental constraints largely because they overlap with the kinematical parameter space of more copiously produced standard model processes. Some of these may be probed by future searches that target the nonexcluded processes detailed in section 5, benefiting as well from the higher energy and luminosity of the LHC.

Acknowledgments

We congratulate our colleagues in the CERN accelerator departments for the excellent performance of the LHC and thank the technical and administrative staffs at CERN and at

JHEP10(2016)129

other CMS institutes for their contributions to the success of the CMS effort. In addition, we gratefully acknowledge the computing centers and personnel of the Worldwide LHC Computing Grid for delivering so effectively the computing infrastructure essential to our analyses. Finally, we acknowledge the enduring support for the construction and operation of the LHC and the CMS detector provided by the following funding agencies: the Austrian Federal Ministry of Science, Research and Economy and the Austrian Science Fund; the Belgian Fonds de la Recherche Scientifique, and Fonds voor Wetenschappelijk Onderzoek; the Brazilian Funding Agencies (CNPq, CAPES, FAPERJ, and FAPESP); the Bulgarian Ministry of Education and Science; CERN; the Chinese Academy of Sciences, Ministry of Science and Technology, and National Natural Science Foundation of China; the Colombian Funding Agency (COLCIENCIAS); the Croatian Ministry of Science, Education and Sport, and the Croatian Science Foundation; the Research Promotion Foundation, Cyprus; the Secretariat for Higher Education, Science, Technology and Innovation, Ecuador; the Ministry of Education and Research, Estonian Research Council via IUT23-4 and IUT23-6 and European Regional Development Fund, Estonia; the Academy of Finland, Finnish Ministry of Education and Culture, and Helsinki Institute of Physics; the Institut National de Physique Nucléaire et de Physique des Particules / CNRS, and Commissariat à l'Énergie Atomique et aux Énergies Alternatives / CEA, France; the Bundesministerium für Bildung und Forschung, Deutsche Forschungsgemeinschaft, and Helmholtz-Gemeinschaft Deutscher Forschungszentren, Germany; the General Secretariat for Research and Technology, Greece; the National Scientific Research Foundation, and National Innovation Office, Hungary; the Department of Atomic Energy and the Department of Science and Technology, India; the Institute for Studies in Theoretical Physics and Mathematics, Iran; the Science Foundation, Ireland; the Istituto Nazionale di Fisica Nucleare, Italy; the Ministry of Science, ICT and Future Planning, and National Research Foundation (NRF), Republic of Korea; the Lithuanian Academy of Sciences; the Ministry of Education, and University of Malaya (Malaysia); the Mexican Funding Agencies (BUAP, CINVESTAV, CONACYT, LNS, SEP, and UASLP-FAI); the Ministry of Business, Innovation and Employment, New Zealand; the Pakistan Atomic Energy Commission; the Ministry of Science and Higher Education and the National Science Centre, Poland; the Fundação para a Ciência e a Tecnologia, Portugal; JINR, Dubna; the Ministry of Education and Science of the Russian Federation, the Federal Agency of Atomic Energy of the Russian Federation, Russian Academy of Sciences, and the Russian Foundation for Basic Research; the Ministry of Education, Science and Technological Development of Serbia; the Secretaría de Estado de Investigación, Desarrollo e Innovación and Programa Consolider-Ingenio 2010, Spain; the Swiss Funding Agencies (ETH Board, ETH Zurich, PSI, SNF, UniZH, Canton Zurich, and SER); the Ministry of Science and Technology, Taipei; the Thailand Center of Excellence in Physics, the Institute for the Promotion of Teaching Science and Technology of Thailand, Special Task Force for Activating Research and the National Science and Technology Development Agency of Thailand; the Scientific and Technical Research Council of Turkey, and Turkish Atomic Energy Authority; the National Academy of Sciences of Ukraine, and State Fund for Fundamental Researches, Ukraine; the Science and Technology Facilities Council, U.K.; the US Department of Energy, and the US National Science Foundation.

JHEP10(2016)129

Individuals have received support from the Marie-Curie program and the European Research Council and EPLANET (European Union); the Leventis Foundation; the A. P. Sloan Foundation; the Alexander von Humboldt Foundation; the Belgian Federal Science Policy Office; the Fonds pour la Formation à la Recherche dans l'Industrie et dans l'Agriculture (FRIA-Belgium); the Agentschap voor Innovatie door Wetenschap en Technologie (IWT-Belgium); the Ministry of Education, Youth and Sports (MEYS) of the Czech Republic; the Council of Science and Industrial Research, India; the HOMING PLUS program of the Foundation for Polish Science, cofinanced from European Union, Regional Development Fund; the Mobility Plus program of the Ministry of Science and Higher Education (Poland); the OPUS program, contract Sonata-bis DEC-2012/07/E/ST2/01406 of the National Science Center (Poland); the Thalis and Aristeia programs cofinanced by EU-ESF and the Greek NSRF; the National Priorities Research Program by Qatar National Research Fund; the Programa Clarín-COFUND del Principado de Asturias; the Rachadapisek Sompot Fund for Postdoctoral Fellowship, Chulalongkorn University (Thailand); the Chulalongkorn Academic into Its 2nd Century Project Advancement Project (Thailand); and the Welch Foundation, contract C-1845.

JHEP10(2016)129

References

[1] P. Ramond, *Dual theory for free fermions*, *Phys. Rev.* **D 3** (1971) 2415 [INSPIRE].

[2] Yu. A. Golfand and E.P. Likhtman, *Extension of the algebra of Poincaré group generators and violation of p invariance*, *JETP Lett.* **13** (1971) 323 [*Pisma Zh. Eksp. Teor. Fiz.* **13** (1971) 452] [INSPIRE].

[3] D.V. Volkov and V.P. Akulov, *Possible universal neutrino interaction*, *JETP Lett.* **16** (1972) 438 [*Pisma Zh. Eksp. Teor. Fiz.* **16** (1972) 621] [INSPIRE].

[4] J. Wess and B. Zumino, *Supergauge transformations in four-dimensions*, *Nucl. Phys.* **B 70** (1974) 39 [INSPIRE].

[5] P. Fayet, *Supergauge invariant extension of the Higgs mechanism and a model for the electron and its neutrino*, *Nucl. Phys.* **B 90** (1975) 104 [INSPIRE].

[6] D.J.H. Chung, L.L. Everett, G.L. Kane, S.F. King, J.D. Lykken and L.-T. Wang, *The soft supersymmetry breaking Lagrangian: theory and applications*, *Phys. Rept.* **407** (2005) 1 [hep-ph/0312378] [INSPIRE].

[7] ATLAS collaboration, *Summary of the searches for squarks and gluinos using $\sqrt{s} = 8$ TeV pp collisions with the ATLAS experiment at the LHC*, *JHEP* **10** (2015) 054 [arXiv:1507.05525] [INSPIRE].

[8] CMS collaboration, *Search for new physics in the multijet and missing transverse momentum final state in proton-proton collisions at $\sqrt{s} = 7$ TeV*, *Phys. Rev. Lett.* **109** (2012) 171803 [arXiv:1207.1898] [INSPIRE].

[9] CMS collaboration, *Search for supersymmetry in events with b-quark jets and missing transverse energy in pp collisions at 7 TeV*, *Phys. Rev.* **D 86** (2012) 072010 [arXiv:1208.4859] [INSPIRE].

[10] CMS collaboration, *Search for electroweak production of charginos and neutralinos using leptonic final states in pp collisions at* $\sqrt{s} = 7$ *TeV*, *JHEP* **11** (2012) 147 [arXiv:1209.6620] [INSPIRE].

[11] CMS collaboration, *Search for new physics in the multijet and missing transverse momentum final state in proton-proton collisions at* $\sqrt{s} = 8$ *TeV*, *JHEP* **06** (2014) 055 [arXiv:1402.4770] [INSPIRE].

[12] CMS collaboration, *Search for supersymmetry in hadronic final states using* M_{T2} *in pp collisions at* $\sqrt{s} = 7$ *TeV*, *JHEP* **10** (2012) 018 [arXiv:1207.1798] [INSPIRE].

[13] CMS collaboration, *Search for gluino mediated bottom- and top-squark production in multijet final states in pp collisions at 8 TeV*, *Phys. Lett.* **B 725** (2013) 243 [arXiv:1305.2390] [INSPIRE].

[14] CMS collaboration, *Search for dark matter, extra dimensions and unparticles in monojet events in proton-proton collisions at* $\sqrt{s} = 8$ *TeV*, *Eur. Phys. J.* **C 75** (2015) 235 [arXiv:1408.3583] [INSPIRE].

[15] CMS collaboration, *Searches for third-generation squark production in fully hadronic final states in proton-proton collisions at* $\sqrt{s} = 8$ *TeV*, *JHEP* **06** (2015) 116 [arXiv:1503.08037] [INSPIRE].

[16] CMS collaboration, *Search for physics beyond the Standard Model in events with two leptons, jets and missing transverse momentum in pp collisions at* $\sqrt{s} = 8$ *TeV*, *JHEP* **04** (2015) 124 [arXiv:1502.06031] [INSPIRE].

[17] CMS collaboration, *Search for new physics in events with same-sign dileptons and jets in pp collisions at* $\sqrt{s} = 8$ *TeV*, *JHEP* **01** (2014) 163 [*Erratum ibid.* **01** (2015) 014] [arXiv:1311.6736] [INSPIRE].

[18] CMS collaboration, *Searches for electroweak production of charginos, neutralinos and sleptons decaying to leptons and W, Z and Higgs bosons in pp collisions at 8 TeV*, *Eur. Phys. J.* **C 74** (2014) 3036 [arXiv:1405.7570] [INSPIRE].

[19] A.H. Chamseddine, R.L. Arnowitt and P. Nath, *Locally supersymmetric grand unification*, *Phys. Rev. Lett.* **49** (1982) 970 [INSPIRE].

[20] R. Barbieri, S. Ferrara and C.A. Savoy, *Gauge models with spontaneously broken local supersymmetry*, *Phys. Lett.* **B 119** (1982) 343 [INSPIRE].

[21] L.E. Ibáñez, *Locally supersymmetric* SU(5) *grand unification*, *Phys. Lett.* **B 118** (1982) 73 [INSPIRE].

[22] L.J. Hall, J.D. Lykken and S. Weinberg, *Supergravity as the messenger of supersymmetry breaking*, *Phys. Rev.* **D 27** (1983) 2359 [INSPIRE].

[23] P. Nath, *Twenty years of SUGRA*, in *Beyond the desert. Proceedings,* 4th *International Conference, Particle physics beyond the standard model, BEYOND* 2003, Castle Ringberg Tegernsee Germany June 9–14 2003, pg. 3 [hep-ph/0307123] [INSPIRE].

[24] G.L. Kane, C.F. Kolda, L. Roszkowski and J.D. Wells, *Study of constrained minimal supersymmetry*, *Phys. Rev.* **D 49** (1994) 6173 [hep-ph/9312272] [INSPIRE].

JHEP10(2016)129

[25] H. Baer, C.-H. Chen, R.B. Munroe, F.E. Paige and X. Tata, *Multichannel search for minimal supergravity at $p\bar{p}$ and e^+e^- colliders*, *Phys. Rev.* **D 51** (1995) 1046 [hep-ph/9408265] [INSPIRE].

[26] J. Alwall, P. Schuster and N. Toro, *Simplified models for a first characterization of new physics at the LHC*, *Phys. Rev.* **D 79** (2009) 075020 [arXiv:0810.3921] [INSPIRE].

[27] LHC New Physics Working Group collaboration, D. Alves, *Simplified models for LHC new physics searches*, *J. Phys.* **G 39** (2012) 105005 [arXiv:1105.2838] [INSPIRE].

[28] CMS collaboration, *Interpretation of searches for supersymmetry with simplified models*, *Phys. Rev.* **D 88** (2013) 052017 [arXiv:1301.2175] [INSPIRE].

[29] MSSM Working Group collaboration, A. Djouadi et al., *The minimal supersymmetric standard model: group summary report*, in *GDR (Groupement De Recherche) — Supersymétrie*, Montpellier France April 15–17 1998 [hep-ph/9901246] [INSPIRE].

[30] G.R. Farrar and S. Weinberg, *Supersymmetry at ordinary energies. 2. R invariance, Goldstone bosons and gauge fermion masses*, *Phys. Rev.* **D 27** (1983) 2732 [INSPIRE].

[31] CMS collaboration, S. Abdullin, P. Azzi, F. Beaudette, P. Janot and A. Perrotta, *The fast simulation of the CMS detector at LHC*, *J. Phys. Conf. Ser.* **331** (2011) 032049 [INSPIRE].

[32] CMS collaboration, S. Banerjee and M.D. Hildreth, *Validation and tuning of the CMS full simulation*, *J. Phys. Conf. Ser.* **331** (2011) 032015 [INSPIRE].

[33] C.P. Robert, *The Bayesian choice: from decision-theoretic foundations to computational implementation*, 2nd edition, Springer Verlag, New York U.S.A. (2007).

[34] A. O'Hagan, *Bayesian inference*, in *Kendall's advanced theory of statistics* **2B**, Edward Arnold, London U.K. (1994).

[35] S. Sekmen et al., *Interpreting LHC SUSY searches in the phenomenological MSSM*, *JHEP* **02** (2012) 075 [arXiv:1109.5119] [INSPIRE].

[36] CMS collaboration, *Search for supersymmetry at the LHC in events with jets and missing transverse energy*, *Phys. Rev. Lett.* **107** (2011) 221804 [arXiv:1109.2352] [INSPIRE].

[37] CMS collaboration, *Search for new physics with same-sign isolated dilepton events with jets and missing transverse energy*, *Phys. Rev. Lett.* **109** (2012) 071803 [arXiv:1205.6615] [INSPIRE].

[38] CMS collaboration, *Search for new physics in events with opposite-sign leptons, jets and missing transverse energy in pp collisions at $\sqrt{s} = 7$ TeV*, *Phys. Lett.* **B 718** (2013) 815 [arXiv:1206.3949] [INSPIRE].

[39] ATLAS collaboration, *Summary of the ATLAS experiment's sensitivity to supersymmetry after LHC run 1 — interpreted in the phenomenological MSSM*, *JHEP* **10** (2015) 134 [arXiv:1508.06608] [INSPIRE].

[40] C.R. Das and M.K. Parida, *New formulas and predictions for running fermion masses at higher scales in SM, 2HDM and MSSM*, *Eur. Phys. J.* **C 20** (2001) 121 [hep-ph/0010004] [INSPIRE].

[41] A.A. Markov, *Extension of the limit theorems of probability theory to a sum of variables connected in a chain*, reprinted in *Dynamic probabilistic systems, volume 1: Markov chains*, appendix B, R. Howard ed., John Wiley and Sons, U.S.A. (1971).

JHEP10(2016)129

[42] N. Metropolis et al., *Equation of state calculations by fast computing machines*, *J. Chem. Phys.* **21** (1953) 1087 [INSPIRE].

[43] W.K. Hastings, *Monte Carlo sampling methods using Markov chains and their applications*, *Biometrika* **57** (1970) 97.

[44] B.A. Berg, *Markov chain Monte Carlo simulations and their statistical analysis*, World Scientific, Singapore (2004).

[45] Heavy Flavor Averaging Group (HFAG) collaboration, Y. Amhis et al., *Averages of b-hadron, c-hadron and τ-lepton properties as of summer* 2014, arXiv:1412.7515 [INSPIRE].

[46] LHCb and CMS collaborations, *Observation of the rare $B_s^0 \to \mu^+\mu^-$ decay from the combined analysis of CMS and LHCb data*, *Nature* **522** (2015) 68 [arXiv:1411.4413] [INSPIRE].

[47] W. Altmannshofer and D.M. Straub, *Viability of MSSM scenarios at very large* $\tan\beta$, *JHEP* **09** (2010) 078 [arXiv:1004.1993] [INSPIRE].

[48] K. Hagiwara, R. Liao, A.D. Martin, D. Nomura and T. Teubner, *$(g-2)_\mu$ and $\alpha(M_Z^2)$ re-evaluated using new precise data*, *J. Phys.* **G 38** (2011) 085003 [arXiv:1105.3149] [INSPIRE].

[49] Particle Data Group collaboration, K.A. Olive et al., *Review of particle physics*, *Chin. Phys.* **C 38** (2014) 090001 [INSPIRE].

[50] Tevatron Electroweak Working Group, CDF and D0 collaborations, T.A. Aaltonen, *Combination of CDF and DO results on the mass of the top quark using up to* 8.7 fb^{-1} *at the Tevatron*, arXiv:1305.3929 [INSPIRE].

[51] J. Bernon, B. Dumont and S. Kraml, *Status of Higgs couplings after run* 1 *of the LHC*, *Phys. Rev.* **D 90** (2014) 071301 [arXiv:1409.1588] [INSPIRE].

[52] J. Bernon and B. Dumont, *Lilith: a tool for constraining new physics from Higgs measurements*, *Eur. Phys. J.* **C 75** (2015) 440 [arXiv:1502.04138] [INSPIRE].

[53] *Joint LEP2 SUSY working group, the ALEPH, DELPHI, L3 and OPAL collaborations webpage*, http://lepsusy.web.cern.ch/lepsusy/.

[54] G. Bélanger, F. Boudjema, A. Pukhov and A. Semenov, *MicrOMEGAs: a program for calculating the relic density in the MSSM*, *Comput. Phys. Commun.* **149** (2002) 103 [hep-ph/0112278] [INSPIRE].

[55] G. Bélanger, F. Boudjema, A. Pukhov and A. Semenov, *MicrOMEGAs: version* 1.3, *Comput. Phys. Commun.* **174** (2006) 577 [hep-ph/0405253] [INSPIRE].

[56] G. Bélanger, F. Boudjema, A. Pukhov and A. Semenov, *Dark matter direct detection rate in a generic model with MicrOMEGAs* 2.2, *Comput. Phys. Commun.* **180** (2009) 747 [arXiv:0803.2360] [INSPIRE].

[57] B.C. Allanach, *SOFTSUSY: a program for calculating supersymmetric spectra*, *Comput. Phys. Commun.* **143** (2002) 305 [hep-ph/0104145] [INSPIRE].

[58] F. Mahmoudi, *SuperIso v*2.3*: a program for calculating flavor physics observables in supersymmetry*, *Comput. Phys. Commun.* **180** (2009) 1579 [arXiv:0808.3144] [INSPIRE].

[59] M. Muhlleitner, A. Djouadi and Y. Mambrini, *SDECAY: a fortran code for the decays of the supersymmetric particles in the MSSM*, *Comput. Phys. Commun.* **168** (2005) 46 [hep-ph/0311167] [INSPIRE].

JHEP10(2016)129

[60] A. Djouadi, J. Kalinowski and M. Spira, *HDECAY: a program for Higgs boson decays in the Standard Model and its supersymmetric extension*, *Comput. Phys. Commun.* **108** (1998) 56 [hep-ph/9704448] [INSPIRE].

[61] ATLAS collaboration, *Updated coupling measurements of the Higgs boson with the ATLAS detector using up to* $25\,\text{fb}^{-1}$ *of proton-proton collision data*, ATLAS-CONF-2014-009, CERN, Geneva Switzerland (2014).

[62] CMS collaboration, *Precise determination of the mass of the Higgs boson and tests of compatibility of its couplings with the Standard Model predictions using proton collisions at* 7 *and* 8 *TeV*, *Eur. Phys. J.* **C 75** (2015) 212 [arXiv:1412.8662] [INSPIRE].

[63] B. Dumont, J.F. Gunion and S. Kraml, *Phenomenological MSSM in view of the* 125 *GeV Higgs data*, *Phys. Rev.* **D 89** (2014) 055018 [arXiv:1312.7027] [INSPIRE].

[64] P.Z. Skands et al., *SUSY Les Houches accord: interfacing SUSY spectrum calculators, decay packages and event generators*, *JHEP* **07** (2004) 036 [hep-ph/0311123] [INSPIRE].

[65] CMS collaboration, *Search for supersymmetry in pp collisions at* $\sqrt{s} = 8$ *TeV in events with a single lepton, large jet multiplicity and multiple b jets*, *Phys. Lett.* **B 733** (2014) 328 [arXiv:1311.4937] [INSPIRE].

[66] CMS collaboration, *Search for top-squark pair production in the single-lepton final state in pp collisions at* $\sqrt{s} = 8$ *TeV*, *Eur. Phys. J.* **C 73** (2013) 2677 [arXiv:1308.1586] [INSPIRE].

[67] S.S. Wilks, *The large-sample distribution of the likelihood ratio for testing composite hypotheses*, *Ann. Math. Statist.* **9** (1938) 60.

[68] T. Sjöstrand, S. Mrenna and P.Z. Skands, *PYTHIA* 6.4 *physics and manual*, *JHEP* **05** (2006) 026 [hep-ph/0603175] [INSPIRE].

[69] M. Cacciari, G.P. Salam and G. Soyez, *The anti-k_t jet clustering algorithm*, *JHEP* **04** (2008) 063 [arXiv:0802.1189] [INSPIRE].

JHEP10(2016)129

The CMS collaboration

Yerevan Physics Institute, Yerevan, Armenia

V. Khachatryan, A.M. Sirunyan, A. Tumasyan

Institut für Hochenergiephysik der OeAW, Wien, Austria

W. Adam, E. Asilar, T. Bergauer, J. Brandstetter, E. Brondolin, M. Dragicevic, J. Erö, M. Flechl, M. Friedl, R. Frühwirth[1], V.M. Ghete, C. Hartl, N. Hörmann, J. Hrubec, M. Jeitler[1], A. König, M. Krammer[1], I. Krätschmer, D. Liko, T. Matsushita, I. Mikulec, D. Rabady, N. Rad, B. Rahbaran, H. Rohringer, J. Schieck[1], R. Schöfbeck, J. Strauss, W. Treberer-Treberspurg, W. Waltenberger, C.-E. Wulz[1]

National Centre for Particle and High Energy Physics, Minsk, Belarus

V. Mossolov, N. Shumeiko, J. Suarez Gonzalez

Universiteit Antwerpen, Antwerpen, Belgium

S. Alderweireldt, T. Cornelis, E.A. De Wolf, X. Janssen, A. Knutsson, J. Lauwers, S. Luyckx, M. Van De Klundert, H. Van Haevermaet, P. Van Mechelen, N. Van Remortel, A. Van Spilbeeck

Vrije Universiteit Brussel, Brussel, Belgium

S. Abu Zeid, F. Blekman, J. D'Hondt, N. Daci, I. De Bruyn, K. Deroover, N. Heracleous, J. Keaveney, S. Lowette, S. Moortgat, L. Moreels, A. Olbrechts, Q. Python, D. Strom, S. Tavernier, W. Van Doninck, P. Van Mulders, G.P. Van Onsem, I. Van Parijs

Université Libre de Bruxelles, Bruxelles, Belgium

H. Brun, C. Caillol, B. Clerbaux, G. De Lentdecker, G. Fasanella, L. Favart, R. Goldouzian, A. Grebenyuk, G. Karapostoli, T. Lenzi, A. Léonard, T. Maerschalk, A. Marinov, L. Perniè, A. Randle-conde, T. Seva, C. Vander Velde, P. Vanlaer, R. Yonamine, F. Zenoni, F. Zhang[2]

Ghent University, Ghent, Belgium

K. Beernaert, L. Benucci, A. Cimmino, S. Crucy, D. Dobur, A. Fagot, G. Garcia, M. Gul, J. Mccartin, A.A. Ocampo Rios, D. Poyraz, D. Ryckbosch, S. Salva, M. Sigamani, M. Tytgat, W. Van Driessche, E. Yazgan, N. Zaganidis

Université Catholique de Louvain, Louvain-la-Neuve, Belgium

S. Basegmez, C. Beluffi[3], O. Bondu, S. Brochet, G. Bruno, A. Caudron, L. Ceard, S. De Visscher, C. Delaere, M. Delcourt, D. Favart, L. Forthomme, A. Giammanco, A. Jafari, P. Jez, M. Komm, V. Lemaitre, A. Mertens, M. Musich, C. Nuttens, L. Perrini, K. Piotrzkowski, L. Quertenmont, M. Selvaggi, M. Vidal Marono

Université de Mons, Mons, Belgium

N. Beliy, G.H. Hammad

Centro Brasileiro de Pesquisas Fisicas, Rio de Janeiro, Brazil

W.L. Aldá Júnior, F.L. Alves, G.A. Alves, L. Brito, M. Correa Martins Junior, M. Hamer, C. Hensel, A. Moraes, M.E. Pol, P. Rebello Teles

JHEP10(2016)129

Universidade do Estado do Rio de Janeiro, Rio de Janeiro, Brazil

E. Belchior Batista Das Chagas, W. Carvalho, J. Chinellato[4], A. Custódio, E.M. Da Costa, D. De Jesus Damiao, C. De Oliveira Martins, S. Fonseca De Souza, L.M. Huertas Guativa, H. Malbouisson, D. Matos Figueiredo, C. Mora Herrera, L. Mundim, H. Nogima, W.L. Prado Da Silva, A. Santoro, A. Sznajder, E.J. Tonelli Manganote[4], A. Vilela Pereira

Universidade Estadual Paulista [a], Universidade Federal do ABC [b], São Paulo, Brazil

S. Ahuja[a], C.A. Bernardes[b], A. De Souza Santos[b], S. Dogra[a], T.R. Fernandez Perez Tomei[a], E.M. Gregores[b], P.G. Mercadante[b], C.S. Moon[a,5], S.F. Novaes[a], Sandra S. Padula[a], D. Romero Abad[b], J.C. Ruiz Vargas

Institute for Nuclear Research and Nuclear Energy, Sofia, Bulgaria

A. Aleksandrov, R. Hadjiiska, P. Iaydjiev, M. Rodozov, S. Stoykova, G. Sultanov, M. Vutova

University of Sofia, Sofia, Bulgaria

A. Dimitrov, I. Glushkov, L. Litov, B. Pavlov, P. Petkov

Beihang University, Beijing, China

W. Fang[6]

Institute of High Energy Physics, Beijing, China

M. Ahmad, J.G. Bian, G.M. Chen, H.S. Chen, M. Chen, T. Cheng, R. Du, C.H. Jiang, D. Leggat, R. Plestina[7], F. Romeo, S.M. Shaheen, A. Spiezia, J. Tao, C. Wang, Z. Wang, H. Zhang

State Key Laboratory of Nuclear Physics and Technology, Peking University, Beijing, China

C. Asawatangtrakuldee, Y. Ban, Q. Li, S. Liu, Y. Mao, S.J. Qian, D. Wang, Z. Xu

Universidad de Los Andes, Bogota, Colombia

C. Avila, A. Cabrera, L.F. Chaparro Sierra, C. Florez, J.P. Gomez, B. Gomez Moreno, J.C. Sanabria

University of Split, Faculty of Electrical Engineering, Mechanical Engineering and Naval Architecture, Split, Croatia

N. Godinovic, D. Lelas, I. Puljak, P.M. Ribeiro Cipriano

University of Split, Faculty of Science, Split, Croatia

Z. Antunovic, M. Kovac

Institute Rudjer Boskovic, Zagreb, Croatia

V. Brigljevic, K. Kadija, J. Luetic, S. Micanovic, L. Sudic

University of Cyprus, Nicosia, Cyprus

A. Attikis, G. Mavromanolakis, J. Mousa, C. Nicolaou, F. Ptochos, P.A. Razis, H. Rykaczewski

JHEP10(2016)129

Charles University, Prague, Czech Republic
M. Finger[8], M. Finger Jr.[8]

Academy of Scientific Research and Technology of the Arab Republic of Egypt, Egyptian Network of High Energy Physics, Cairo, Egypt
T. Elkafrawy[9], M.A. Mahmoud[10,11], Y. Mohammed[10]

National Institute of Chemical Physics and Biophysics, Tallinn, Estonia
B. Calpas, M. Kadastik, M. Murumaa, M. Raidal, A. Tiko, C. Veelken

Department of Physics, University of Helsinki, Helsinki, Finland
P. Eerola, J. Pekkanen, M. Voutilainen

Helsinki Institute of Physics, Helsinki, Finland
J. Härkönen, V. Karimäki, R. Kinnunen, T. Lampén, K. Lassila-Perini, S. Lehti, T. Lindén, P. Luukka, T. Peltola, J. Tuominiemi, E. Tuovinen, L. Wendland

Lappeenranta University of Technology, Lappeenranta, Finland
J. Talvitie, T. Tuuva

DSM/IRFU, CEA/Saclay, Gif-sur-Yvette, France
M. Besancon, F. Couderc, M. Dejardin, D. Denegri, B. Fabbro, J.L. Faure, C. Favaro, F. Ferri, S. Ganjour, A. Givernaud, P. Gras, G. Hamel de Monchenault, P. Jarry, E. Locci, M. Machet, J. Malcles, J. Rander, A. Rosowsky, M. Titov, A. Zghiche

Laboratoire Leprince-Ringuet, Ecole Polytechnique, IN2P3-CNRS, Palaiseau, France
A. Abdulsalam, I. Antropov, S. Baffioni, F. Beaudette, P. Busson, L. Cadamuro, E. Chapon, C. Charlot, O. Davignon, N. Filipovic, R. Granier de Cassagnac, M. Jo, S. Kraml, S. Lisniak, P. Miné, I.N. Naranjo, M. Nguyen, C. Ochando, G. Ortona, P. Paganini, P. Pigard, S. Regnard, R. Salerno, Y. Sirois, T. Strebler, Y. Yilmaz, A. Zabi

Institut Pluridisciplinaire Hubert Curien, Université de Strasbourg, Université de Haute Alsace Mulhouse, CNRS/IN2P3, Strasbourg, France
J.-L. Agram[12], J. Andrea, A. Aubin, D. Bloch, J.-M. Brom, M. Buttignol, E.C. Chabert, N. Chanon, C. Collard, E. Conte[12], X. Coubez, J.-C. Fontaine[12], D. Gelé, U. Goerlach, C. Goetzmann, A.-C. Le Bihan, J.A. Merlin[13], K. Skovpen, P. Van Hove

Centre de Calcul de l'Institut National de Physique Nucleaire et de Physique des Particules, CNRS/IN2P3, Villeurbanne, France
S. Gadrat

Université de Lyon, Université Claude Bernard Lyon 1, CNRS-IN2P3, Institut de Physique Nucléaire de Lyon, Villeurbanne, France
S. Beauceron, C. Bernet, G. Boudoul, E. Bouvier, C.A. Carrillo Montoya, R. Chierici, D. Contardo, B. Courbon, P. Depasse, H. El Mamouni, J. Fan, J. Fay, S. Gascon, M. Gouzevitch, B. Ille, F. Lagarde, I.B. Laktineh, M. Lethuillier, L. Mirabito, A.L. Pequegnot, S. Perries, A. Popov[14], J.D. Ruiz Alvarez, D. Sabes, V. Sordini, M. Vander Donckt, P. Verdier, S. Viret

JHEP10(2016)129

Georgian Technical University, Tbilisi, Georgia
T. Toriashvili[15]

Tbilisi State University, Tbilisi, Georgia
Z. Tsamalaidze[8]

RWTH Aachen University, I. Physikalisches Institut, Aachen, Germany
C. Autermann, S. Beranek, L. Feld, A. Heister, M.K. Kiesel, K. Klein, M. Lipinski, A. Ostapchuk, M. Preuten, F. Raupach, S. Schael, J.F. Schulte, T. Verlage, H. Weber, V. Zhukov[14]

RWTH Aachen University, III. Physikalisches Institut A, Aachen, Germany
M. Ata, M. Brodski, E. Dietz-Laursonn, D. Duchardt, M. Endres, M. Erdmann, S. Erdweg, T. Esch, R. Fischer, A. Güth, T. Hebbeker, C. Heidemann, K. Hoepfner, S. Knutzen, M. Merschmeyer, A. Meyer, P. Millet, S. Mukherjee, M. Olschewski, K. Padeken, P. Papacz, T. Pook, M. Radziej, H. Reithler, M. Rieger, F. Scheuch, L. Sonnenschein, D. Teyssier, S. Thüer

RWTH Aachen University, III. Physikalisches Institut B, Aachen, Germany
V. Cherepanov, Y. Erdogan, G. Flügge, H. Geenen, M. Geisler, F. Hoehle, B. Kargoll, T. Kress, A. Künsken, J. Lingemann, A. Nehrkorn, A. Nowack, I.M. Nugent, C. Pistone, O. Pooth, A. Stahl[13]

Deutsches Elektronen-Synchrotron, Hamburg, Germany
M. Aldaya Martin, I. Asin, N. Bartosik, O. Behnke, U. Behrens, K. Borras[16], A. Burgmeier, A. Campbell, C. Contreras-Campana, F. Costanza, C. Diez Pardos, G. Dolinska, S. Dooling, T. Dorland, G. Eckerlin, D. Eckstein, T. Eichhorn, G. Flucke, E. Gallo[17], J. Garay Garcia, A. Geiser, A. Gizhko, P. Gunnellini, J. Hauk, M. Hempel[18], H. Jung, A. Kalogeropoulos, O. Karacheban[18], M. Kasemann, P. Katsas, J. Kieseler, C. Kleinwort, I. Korol, W. Lange, J. Leonard, K. Lipka, A. Lobanov, W. Lohmann[18], R. Mankel, I.-A. Melzer-Pellmann, A.B. Meyer, G. Mittag, J. Mnich, A. Mussgiller, S. Naumann-Emme, A. Nayak, E. Ntomari, H. Perrey, D. Pitzl, R. Placakyte, A. Raspereza, B. Roland, M.Ö. Sahin, P. Saxena, T. Schoerner-Sadenius, C. Seitz, S. Spannagel, N. Stefaniuk, K.D. Trippkewitz, R. Walsh, C. Wissing

University of Hamburg, Hamburg, Germany
V. Blobel, M. Centis Vignali, A.R. Draeger, T. Dreyer, J. Erfle, E. Garutti, K. Goebel, D. Gonzalez, M. Görner, J. Haller, M. Hoffmann, R.S. Höing, A. Junkes, R. Klanner, R. Kogler, N. Kovalchuk, T. Lapsien, T. Lenz, I. Marchesini, D. Marconi, M. Meyer, M. Niedziela, D. Nowatschin, J. Ott, F. Pantaleo[13], T. Peiffer, A. Perieanu, N. Pietsch, J. Poehlsen, C. Sander, C. Scharf, P. Schleper, E. Schlieckau, A. Schmidt, S. Schumann, J. Schwandt, V. Sola, H. Stadie, G. Steinbrück, F.M. Stober, H. Tholen, D. Troendle, E. Usai, L. Vanelderen, A. Vanhoefer, B. Vormwald

Institut für Experimentelle Kernphysik, Karlsruhe, Germany
C. Barth, C. Baus, J. Berger, C. Böser, E. Butz, T. Chwalek, F. Colombo, W. De Boer, A. Descroix, A. Dierlamm, S. Fink, F. Frensch, R. Friese, M. Giffels, A. Gilbert, D. Haitz,

JHEP10(2016)129

F. Hartmann[13], S.M. Heindl, U. Husemann, I. Katkov[14], A. Kornmayer[13], P. Lobelle Pardo, B. Maier, H. Mildner, M.U. Mozer, T. Müller, Th. Müller, M. Plagge, G. Quast, K. Rabbertz, S. Röcker, F. Roscher, M. Schröder, G. Sieber, H.J. Simonis, R. Ulrich, J. Wagner-Kuhr, S. Wayand, M. Weber, T. Weiler, S. Williamson, C. Wöhrmann, R. Wolf

Institute of Nuclear and Particle Physics (INPP), NCSR Demokritos, Aghia Paraskevi, Greece

G. Anagnostou, G. Daskalakis, T. Geralis, V.A. Giakoumopoulou, A. Kyriakis, D. Loukas, A. Psallidas, I. Topsis-Giotis

National and Kapodistrian University of Athens, Athens, Greece

A. Agapitos, S. Kesisoglou, A. Panagiotou, N. Saoulidou, E. Tziaferi

University of Ioánnina, Ioánnina, Greece

I. Evangelou, G. Flouris, C. Foudas, P. Kokkas, N. Loukas, N. Manthos, I. Papadopoulos, E. Paradas, J. Strologas

Wigner Research Centre for Physics, Budapest, Hungary

G. Bencze, C. Hajdu, P. Hidas, D. Horvath[19], F. Sikler, V. Veszpremi, G. Vesztergombi[20], A.J. Zsigmond

Institute of Nuclear Research ATOMKI, Debrecen, Hungary

N. Beni, S. Czellar, J. Karancsi[21], J. Molnar, Z. Szillasi

University of Debrecen, Debrecen, Hungary

M. Bartók[20], A. Makovec, P. Raics, Z.L. Trocsanyi, B. Ujvari

National Institute of Science Education and Research, Bhubaneswar, India

S. Choudhury[22], P. Mal, K. Mandal, D.K. Sahoo, N. Sahoo, S.K. Swain

Panjab University, Chandigarh, India

S. Bansal, S.B. Beri, V. Bhatnagar, R. Chawla, R. Gupta, U.Bhawandeep, A.K. Kalsi, A. Kaur, M. Kaur, R. Kumar, A. Mehta, M. Mittal, J.B. Singh, G. Walia

University of Delhi, Delhi, India

Ashok Kumar, A. Bhardwaj, B.C. Choudhary, R.B. Garg, S. Keshri, A. Kumar, S. Malhotra, M. Naimuddin, N. Nishu, K. Ranjan, R. Sharma, V. Sharma

Saha Institute of Nuclear Physics, Kolkata, India

R. Bhattacharya, S. Bhattacharya, K. Chatterjee, S. Dey, S. Dutta, S. Ghosh, N. Majumdar, A. Modak, K. Mondal, S. Mukhopadhyay, S. Nandan, A. Purohit, A. Roy, D. Roy, S. Roy Chowdhury, S. Sarkar, M. Sharan

Bhabha Atomic Research Centre, Mumbai, India

R. Chudasama, D. Dutta, V. Jha, V. Kumar, A.K. Mohanty[13], L.M. Pant, P. Shukla, A. Topkar

Tata Institute of Fundamental Research, Mumbai, India

T. Aziz, S. Banerjee, S. Bhowmik[23], R.M. Chatterjee, R.K. Dewanjee, S. Dugad, S. Ganguly, S. Ghosh, M. Guchait, A. Gurtu[24], Sa. Jain, G. Kole, S. Kumar, B. Mahakud,

JHEP10(2016)129

M. Maity[23], G. Majumder, K. Mazumdar, S. Mitra, G.B. Mohanty, B. Parida, T. Sarkar[23], N. Sur, B. Sutar, N. Wickramage[25]

Indian Institute of Science Education and Research (IISER), Pune, India

S. Chauhan, S. Dube, A. Kapoor, K. Kothekar, A. Rane, S. Sharma

Institute for Research in Fundamental Sciences (IPM), Tehran, Iran

H. Bakhshiansohi, H. Behnamian, S.M. Etesami[26], A. Fahim[27], M. Khakzad, M. Mohammadi Najafabadi, M. Naseri, S. Paktinat Mehdiabadi, F. Rezaei Hosseinabadi, B. Safarzadeh[28], M. Zeinali

University College Dublin, Dublin, Ireland

M. Felcini, M. Grunewald

INFN Sezione di Bari [a], Università di Bari [b], Politecnico di Bari [c], Bari, Italy

M. Abbrescia[a,b], C. Calabria[a,b], C. Caputo[a,b], A. Colaleo[a], D. Creanza[a,c], L. Cristella[a,b], N. De Filippis[a,c], M. De Palma[a,b], L. Fiore[a], G. Iaselli[a,c], G. Maggi[a,c], M. Maggi[a], G. Miniello[a,b], S. My[a,b], S. Nuzzo[a,b], A. Pompili[a,b], G. Pugliese[a,c], R. Radogna[a,b], A. Ranieri[a], G. Selvaggi[a,b], L. Silvestris[a,13], R. Venditti[a,b]

INFN Sezione di Bologna [a], Università di Bologna [b], Bologna, Italy

G. Abbiendi[a], C. Battilana[13], D. Bonacorsi[a,b], S. Braibant-Giacomelli[a,b], L. Brigliadori[a,b], R. Campanini[a,b], P. Capiluppi[a,b], A. Castro[a,b], F.R. Cavallo[a], S.S. Chhibra[a,b], G. Codispoti[a,b], M. Cuffiani[a,b], G.M. Dallavalle[a], F. Fabbri[a], A. Fanfani[a,b], D. Fasanella[a,b], P. Giacomelli[a], C. Grandi[a], L. Guiducci[a,b], S. Marcellini[a], G. Masetti[a], A. Montanari[a], F.L. Navarria[a,b], A. Perrotta[a], A.M. Rossi[a,b], T. Rovelli[a,b], G.P. Siroli[a,b], N. Tosi[a,b,13]

INFN Sezione di Catania [a], Università di Catania [b], Catania, Italy

G. Cappello[b], M. Chiorboli[a,b], S. Costa[a,b], A. Di Mattia[a], F. Giordano[a,b], R. Potenza[a,b], A. Tricomi[a,b], C. Tuve[a,b]

INFN Sezione di Firenze [a], Università di Firenze [b], Firenze, Italy

G. Barbagli[a], V. Ciulli[a,b], C. Civinini[a], R. D'Alessandro[a,b], E. Focardi[a,b], V. Gori[a,b], P. Lenzi[a,b], M. Meschini[a], S. Paoletti[a], G. Sguazzoni[a], L. Viliani[a,b,13]

INFN Laboratori Nazionali di Frascati, Frascati, Italy

L. Benussi, S. Bianco, F. Fabbri, D. Piccolo, F. Primavera[13]

INFN Sezione di Genova [a], Università di Genova [b], Genova, Italy

V. Calvelli[a,b], F. Ferro[a], M. Lo Vetere[a,b], M.R. Monge[a,b], E. Robutti[a], S. Tosi[a,b]

INFN Sezione di Milano-Bicocca [a], Università di Milano-Bicocca [b], Milano, Italy

L. Brianza, M.E. Dinardo[a,b], S. Fiorendi[a,b], S. Gennai[a], R. Gerosa[a,b], A. Ghezzi[a,b], P. Govoni[a,b], S. Malvezzi[a], R.A. Manzoni[a,b,13], B. Marzocchi[a,b], D. Menasce[a], L. Moroni[a], M. Paganoni[a,b], D. Pedrini[a], S. Pigazzini, S. Ragazzi[a,b], N. Redaelli[a], T. Tabarelli de Fatis[a,b]

JHEP10(2016)129

INFN Sezione di Napoli [a], Università di Napoli 'Federico II' [b], Napoli, Italy, Università della Basilicata [c], Potenza, Italy, Università G. Marconi [d], Roma, Italy

S. Buontempo[a], N. Cavallo[a,c], S. Di Guida[a,d,13], M. Esposito[a,b], F. Fabozzi[a,c], A.O.M. Iorio[a,b], G. Lanza[a], L. Lista[a], S. Meola[a,d,13], M. Merola[a], P. Paolucci[a,13], C. Sciacca[a,b], F. Thyssen

INFN Sezione di Padova [a], Università di Padova [b], Padova, Italy, Università di Trento [c], Trento, Italy

P. Azzi[a,13], N. Bacchetta[a], L. Benato[a,b], D. Bisello[a,b], A. Boletti[a,b], A. Branca[a,b], R. Carlin[a,b], P. Checchia[a], M. Dall'Osso[a,b,13], T. Dorigo[a], U. Dosselli[a], F. Gasparini[a,b], U. Gasparini[a,b], A. Gozzelino[a], K. Kanishchev[a,c], S. Lacaprara[a], M. Margoni[a,b], A.T. Meneguzzo[a,b], J. Pazzini[a,b,13], N. Pozzobon[a,b], P. Ronchese[a,b], F. Simonetto[a,b], E. Torassa[a], M. Tosi[a,b], S. Ventura[a], M. Zanetti, P. Zotto[a,b], A. Zucchetta[a,b,13], G. Zumerle[a,b]

INFN Sezione di Pavia [a], Università di Pavia [b], Pavia, Italy

A. Braghieri[a], A. Magnani[a,b], P. Montagna[a,b], S.P. Ratti[a,b], V. Re[a], C. Riccardi[a,b], P. Salvini[a], I. Vai[a,b], P. Vitulo[a,b]

INFN Sezione di Perugia [a], Università di Perugia [b], Perugia, Italy

L. Alunni Solestizi[a,b], G.M. Bilei[a], D. Ciangottini[a,b], L. Fanò[a,b], P. Lariccia[a,b], G. Mantovani[a,b], M. Menichelli[a], A. Saha[a], A. Santocchia[a,b]

INFN Sezione di Pisa [a], Università di Pisa [b], Scuola Normale Superiore di Pisa [c], Pisa, Italy

K. Androsov[a,29], P. Azzurri[a,13], G. Bagliesi[a], J. Bernardini[a], T. Boccali[a], R. Castaldi[a], M.A. Ciocci[a,29], R. Dell'Orso[a], S. Donato[a,c], G. Fedi, L. Foà[a,c†], A. Giassi[a], M.T. Grippo[a,29], F. Ligabue[a,c], T. Lomtadze[a], L. Martini[a,b], A. Messineo[a,b], F. Palla[a], A. Rizzi[a,b], A. Savoy-Navarro[a,30], P. Spagnolo[a], R. Tenchini[a], G. Tonelli[a,b], A. Venturi[a], P.G. Verdini[a]

INFN Sezione di Roma [a], Università di Roma [b], Roma, Italy

L. Barone[a,b], F. Cavallari[a], G. D'imperio[a,b,13], D. Del Re[a,b,13], M. Diemoz[a], S. Gelli[a,b], C. Jorda[a], E. Longo[a,b], F. Margaroli[a,b], P. Meridiani[a], G. Organtini[a,b], R. Paramatti[a], F. Preiato[a,b], S. Rahatlou[a,b], C. Rovelli[a], F. Santanastasio[a,b]

INFN Sezione di Torino [a], Università di Torino [b], Torino, Italy, Università del Piemonte Orientale [c], Novara, Italy

N. Amapane[a,b], R. Arcidiacono[a,c,13], S. Argiro[a,b], M. Arneodo[a,c], R. Bellan[a,b], C. Biino[a], N. Cartiglia[a], M. Costa[a,b], R. Covarelli[a,b], A. Degano[a,b], N. Demaria[a], L. Finco[a,b], B. Kiani[a,b], C. Mariotti[a], S. Maselli[a], E. Migliore[a,b], V. Monaco[a,b], E. Monteil[a,b], M.M. Obertino[a,b], L. Pacher[a,b], N. Pastrone[a], M. Pelliccioni[a], G.L. Pinna Angioni[a,b], F. Ravera[a,b], A. Romero[a,b], M. Ruspa[a,c], R. Sacchi[a,b], A. Solano[a,b], A. Staiano[a]

JHEP10(2016)129

INFN Sezione di Trieste [a], Università di Trieste [b], Trieste, Italy
S. Belforte[a], V. Candelise[a,b], M. Casarsa[a], F. Cossutti[a], G. Della Ricca[a,b], B. Gobbo[a], C. La Licata[a,b], A. Schizzi[a,b], A. Zanetti[a]

Kangwon National University, Chunchon, Korea
A. Kropivnitskaya, S.K. Nam

Kyungpook National University, Daegu, Korea
D.H. Kim, G.N. Kim, M.S. Kim, D.J. Kong, S. Lee, S.W. Lee, Y.D. Oh, A. Sakharov, S. Sekmen, D.C. Son

Chonbuk National University, Jeonju, Korea
J.A. Brochero Cifuentes, H. Kim, T.J. Kim[31]

Chonnam National University, Institute for Universe and Elementary Particles, Kwangju, Korea
S. Song

Korea University, Seoul, Korea
S. Cho, S. Choi, Y. Go, D. Gyun, B. Hong, H. Kim, Y. Kim, B. Lee, K. Lee, K.S. Lee, S. Lee, J. Lim, S.K. Park, Y. Roh

Seoul National University, Seoul, Korea
H.D. Yoo

University of Seoul, Seoul, Korea
M. Choi, H. Kim, J.H. Kim, J.S.H. Lee, I.C. Park, G. Ryu, M.S. Ryu

Sungkyunkwan University, Suwon, Korea
Y. Choi, J. Goh, D. Kim, E. Kwon, J. Lee, I. Yu

Vilnius University, Vilnius, Lithuania
V. Dudenas, A. Juodagalvis, J. Vaitkus

National Centre for Particle Physics, Universiti Malaya, Kuala Lumpur, Malaysia
I. Ahmed, Z.A. Ibrahim, J.R. Komaragiri, M.A.B. Md Ali[32], F. Mohamad Idris[33], W.A.T. Wan Abdullah, M.N. Yusli, Z. Zolkapli

Centro de Investigacion y de Estudios Avanzados del IPN, Mexico City, Mexico
E. Casimiro Linares, H. Castilla-Valdez, E. De La Cruz-Burelo, I. Heredia-De La Cruz[34], A. Hernandez-Almada, R. Lopez-Fernandez, J. Mejia Guisao, A. Sanchez-Hernandez

Universidad Iberoamericana, Mexico City, Mexico
S. Carrillo Moreno, F. Vazquez Valencia

Benemerita Universidad Autonoma de Puebla, Puebla, Mexico
I. Pedraza, H.A. Salazar Ibarguen

Universidad Autónoma de San Luis Potosí, San Luis Potosí, Mexico
A. Morelos Pineda

JHEP10(2016)129

University of Auckland, Auckland, New Zealand
D. Krofcheck

University of Canterbury, Christchurch, New Zealand
P.H. Butler

National Centre for Physics, Quaid-I-Azam University, Islamabad, Pakistan
A. Ahmad, M. Ahmad, Q. Hassan, H.R. Hoorani, W.A. Khan, T. Khurshid, M. Shoaib, M. Waqas

National Centre for Nuclear Research, Swierk, Poland
H. Bialkowska, M. Bluj, B. Boimska, T. Frueboes, M. Górski, M. Kazana, K. Nawrocki, K. Romanowska-Rybinska, M. Szleper, P. Traczyk, P. Zalewski

Institute of Experimental Physics, Faculty of Physics, University of Warsaw, Warsaw, Poland
G. Brona, K. Bunkowski, A. Byszuk[35], K. Doroba, A. Kalinowski, M. Konecki, J. Krolikowski, M. Misiura, M. Olszewski, M. Walczak

Laboratório de Instrumentação e Física Experimental de Partículas, Lisboa, Portugal
P. Bargassa, C. Beirão Da Cruz E Silva, A. Di Francesco, P. Faccioli, P.G. Ferreira Parracho, M. Gallinaro, J. Hollar, N. Leonardo, L. Lloret Iglesias, M.V. Nemallapudi, F. Nguyen, J. Rodrigues Antunes, J. Seixas, O. Toldaiev, D. Vadruccio, J. Varela, P. Vischia

Joint Institute for Nuclear Research, Dubna, Russia
P. Bunin, M. Gavrilenko, I. Golutvin, I. Gorbunov, A. Kamenev, V. Karjavin, A. Lanev, A. Malakhov, V. Matveev[36,37], P. Moisenz, V. Palichik, V. Perelygin, M. Savina, S. Shmatov, S. Shulha, N. Skatchkov, V. Smirnov, N. Voytishin, A. Zarubin

Petersburg Nuclear Physics Institute, Gatchina (St. Petersburg), Russia
V. Golovtsov, Y. Ivanov, V. Kim[38], E. Kuznetsova, P. Levchenko, V. Murzin, V. Oreshkin, I. Smirnov, V. Sulimov, L. Uvarov, S. Vavilov, A. Vorobyev

Institute for Nuclear Research, Moscow, Russia
Yu. Andreev, A. Dermenev, S. Gninenko, N. Golubev, A. Karneyeu, M. Kirsanov, N. Krasnikov, A. Pashenkov, D. Tlisov, A. Toropin

Institute for Theoretical and Experimental Physics, Moscow, Russia
V. Epshteyn, V. Gavrilov, N. Lychkovskaya, V. Popov, I. Pozdnyakov, G. Safronov, A. Spiridonov, E. Vlasov, A. Zhokin

National Research Nuclear University 'Moscow Engineering Physics Institute' (MEPhI), Moscow, Russia
M. Chadeeva, M. Danilov, O. Markin, V. Rusinov, E. Tarkovskii

P.N. Lebedev Physical Institute, Moscow, Russia
V. Andreev, M. Azarkin[37], I. Dremin[37], M. Kirakosyan, A. Leonidov[37], G. Mesyats, S.V. Rusakov

JHEP10(2016)129

Skobeltsyn Institute of Nuclear Physics, Lomonosov Moscow State University, Moscow, Russia

A. Baskakov, A. Belyaev, E. Boos, M. Dubinin[39], L. Dudko, A. Ershov, A. Gribushin, V. Klyukhin, O. Kodolova, I. Lokhtin, I. Miagkov, S. Obraztsov, S. Petrushanko, V. Savrin, A. Snigirev

State Research Center of Russian Federation, Institute for High Energy Physics, Protvino, Russia

I. Azhgirey, I. Bayshev, S. Bitioukov, V. Kachanov, A. Kalinin, D. Konstantinov, V. Krychkine, V. Petrov, R. Ryutin, A. Sobol, L. Tourtchanovitch, S. Troshin, N. Tyurin, A. Uzunian, A. Volkov

University of Belgrade, Faculty of Physics and Vinca Institute of Nuclear Sciences, Belgrade, Serbia

P. Adzic[40], P. Cirkovic, D. Devetak, J. Milosevic, V. Rekovic

Centro de Investigaciones Energéticas Medioambientales y Tecnológicas (CIEMAT), Madrid, Spain

J. Alcaraz Maestre, E. Calvo, M. Cerrada, M. Chamizo Llatas, N. Colino, B. De La Cruz, A. Delgado Peris, A. Escalante Del Valle, C. Fernandez Bedoya, J.P. Fernández Ramos, J. Flix, M.C. Fouz, P. Garcia-Abia, O. Gonzalez Lopez, S. Goy Lopez, J.M. Hernandez, M.I. Josa, E. Navarro De Martino, A. Pérez-Calero Yzquierdo, J. Puerta Pelayo, A. Quintario Olmeda, I. Redondo, L. Romero, M.S. Soares

Universidad Autónoma de Madrid, Madrid, Spain

J.F. de Trocóniz, M. Missiroli, D. Moran

Universidad de Oviedo, Oviedo, Spain

J. Cuevas, J. Fernandez Menendez, S. Folgueras, I. Gonzalez Caballero, E. Palencia Cortezon[13], J.M. Vizan Garcia

Instituto de Física de Cantabria (IFCA), CSIC-Universidad de Cantabria, Santander, Spain

I.J. Cabrillo, A. Calderon, J.R. Castiñeiras De Saa, E. Curras, P. De Castro Manzano, M. Fernandez, J. Garcia-Ferrero, G. Gomez, A. Lopez Virto, J. Marco, R. Marco, C. Martinez Rivero, F. Matorras, J. Piedra Gomez, T. Rodrigo, A.Y. Rodríguez-Marrero, A. Ruiz-Jimeno, L. Scodellaro, N. Trevisani, I. Vila, R. Vilar Cortabitarte

CERN, European Organization for Nuclear Research, Geneva, Switzerland

D. Abbaneo, E. Auffray, G. Auzinger, M. Bachtis, P. Baillon, A.H. Ball, D. Barney, A. Benaglia, L. Benhabib, G.M. Berruti, P. Bloch, A. Bocci, A. Bonato, C. Botta, H. Breuker, T. Camporesi, R. Castello, M. Cepeda, G. Cerminara, M. D'Alfonso, D. d'Enterria, A. Dabrowski, V. Daponte, A. David, M. De Gruttola, F. De Guio, A. De Roeck, E. Di Marco[41], M. Dobson, M. Dordevic, B. Dorney, T. du Pree, D. Duggan, M. Dünser, N. Dupont, A. Elliott-Peisert, G. Franzoni, J. Fulcher, W. Funk, D. Gigi, K. Gill, M. Girone, F. Glege, R. Guida, S. Gundacker, M. Guthoff, J. Hammer, P. Harris, J. Hegeman, V. Innocente, P. Janot, H. Kirschenmann, V. Knünz, M.J. Kortelainen, K. Kousouris,

JHEP10(2016)129

P. Lecoq, C. Lourenço, M.T. Lucchini, N. Magini, L. Malgeri, M. Mannelli, A. Martelli, L. Masetti, F. Meijers, S. Mersi, E. Meschi, F. Moortgat, S. Morovic, M. Mulders, H. Neugebauer, S. Orfanelli[42], L. Orsini, L. Pape, E. Perez, M. Peruzzi, A. Petrilli, G. Petrucciani, A. Pfeiffer, M. Pierini, D. Piparo, A. Racz, T. Reis, G. Rolandi[43], M. Rovere, M. Ruan, H. Sakulin, J.B. Sauvan, C. Schäfer, C. Schwick, M. Seidel, A. Sharma, P. Silva, M. Simon, P. Sphicas[44], J. Steggemann, M. Stoye, Y. Takahashi, D. Treille, A. Triossi, A. Tsirou, G.I. Veres[20], N. Wardle, H.K. Wöhri, A. Zagozdzinska[35], W.D. Zeuner

Paul Scherrer Institut, Villigen, Switzerland

W. Bertl, K. Deiters, W. Erdmann, R. Horisberger, Q. Ingram, H.C. Kaestli, D. Kotlinski, U. Langenegger, T. Rohe

Institute for Particle Physics, ETH Zurich, Zurich, Switzerland

F. Bachmair, L. Bäni, L. Bianchini, B. Casal, G. Dissertori, M. Dittmar, M. Donegà, P. Eller, C. Grab, C. Heidegger, D. Hits, J. Hoss, G. Kasieczka, P. Lecomte†, W. Lustermann, B. Mangano, M. Marionneau, P. Martinez Ruiz del Arbol, M. Masciovecchio, M.T. Meinhard, D. Meister, F. Micheli, P. Musella, F. Nessi-Tedaldi, F. Pandolfi, J. Pata, F. Pauss, G. Perrin, L. Perrozzi, M. Quittnat, M. Rossini, M. Schönenberger, A. Starodumov[45], M. Takahashi, V.R. Tavolaro, K. Theofilatos, R. Wallny

Universität Zürich, Zurich, Switzerland

T.K. Aarrestad, C. Amsler[46], L. Caminada, M.F. Canelli, V. Chiochia, A. De Cosa, C. Galloni, A. Hinzmann, T. Hreus, B. Kilminster, C. Lange, J. Ngadiuba, D. Pinna, G. Rauco, P. Robmann, D. Salerno, Y. Yang

National Central University, Chung-Li, Taiwan

K.H. Chen, T.H. Doan, Sh. Jain, R. Khurana, M. Konyushikhin, C.M. Kuo, W. Lin, Y.J. Lu, A. Pozdnyakov, S.S. Yu

National Taiwan University (NTU), Taipei, Taiwan

Arun Kumar, P. Chang, Y.H. Chang, Y.W. Chang, Y. Chao, K.F. Chen, P.H. Chen, C. Dietz, F. Fiori, U. Grundler, W.-S. Hou, Y. Hsiung, Y.F. Liu, R.-S. Lu, M. Miñano Moya, E. Petrakou, J.f. Tsai, Y.M. Tzeng

Chulalongkorn University, Faculty of Science, Department of Physics, Bangkok, Thailand

B. Asavapibhop, K. Kovitanggoon, G. Singh, N. Srimanobhas, N. Suwonjandee

Cukurova University, Adana, Turkey

A. Adiguzel, S. Cerci[47], S. Damarseckin, Z.S. Demiroglu, C. Dozen, I. Dumanoglu, S. Girgis, G. Gokbulut, Y. Guler, E. Gurpinar, I. Hos, E.E. Kangal[48], A. Kayis Topaksu, G. Onengut[49], K. Ozdemir[50], S. Ozturk[51], B. Tali[47], H. Topakli[51], C. Zorbilmez

Middle East Technical University, Physics Department, Ankara, Turkey

B. Bilin, S. Bilmis, B. Isildak[52], G. Karapinar[53], M. Yalvac, M. Zeyrek

Bogazici University, Istanbul, Turkey

E. Gülmez, M. Kaya[54], O. Kaya[55], E.A. Yetkin[56], T. Yetkin[57]

JHEP10(2016)129

Istanbul Technical University, Istanbul, Turkey
A. Cakir, K. Cankocak, S. Sen[58], F.I. Vardarlı

Institute for Scintillation Materials of National Academy of Science of Ukraine, Kharkov, Ukraine
B. Grynyov

National Scientific Center, Kharkov Institute of Physics and Technology, Kharkov, Ukraine
L. Levchuk, P. Sorokin

University of Bristol, Bristol, United Kingdom
R. Aggleton, F. Ball, L. Beck, J.J. Brooke, D. Burns, E. Clement, D. Cussans, H. Flacher, J. Goldstein, M. Grimes, G.P. Heath, H.F. Heath, J. Jacob, L. Kreczko, C. Lucas, Z. Meng, D.M. Newbold[59], S. Paramesvaran, A. Poll, T. Sakuma, S. Seif El Nasr-storey, S. Senkin, D. Smith, V.J. Smith

Rutherford Appleton Laboratory, Didcot, United Kingdom
K.W. Bell, A. Belyaev[60], C. Brew, R.M. Brown, L. Calligaris, D. Cieri, D.J.A. Cockerill, J.A. Coughlan, K. Harder, S. Harper, E. Olaiya, D. Petyt, C.H. Shepherd-Themistocleous, A. Thea, I.R. Tomalin, T. Williams, S.D. Worm

Imperial College, London, United Kingdom
M. Baber, R. Bainbridge, O. Buchmuller, A. Bundock, D. Burton, S. Casasso, M. Citron, D. Colling, L. Corpe, P. Dauncey, G. Davies, A. De Wit, M. Della Negra, P. Dunne, A. Elwood, D. Futyan, G. Hall, G. Iles, R. Lane, R. Lucas[59], L. Lyons, A.-M. Magnan, S. Malik, L. Mastrolorenzo, J. Nash, A. Nikitenko[45], J. Pela, B. Penning, M. Pesaresi, D.M. Raymond, A. Richards, A. Rose, C. Seez, A. Tapper, K. Uchida, M. Vazquez Acosta[61], T. Virdee[13], S.C. Zenz

Brunel University, Uxbridge, United Kingdom
J.E. Cole, P.R. Hobson, A. Khan, P. Kyberd, D. Leslie, I.D. Reid, P. Symonds, L. Teodorescu, M. Turner

Baylor University, Waco, U.S.A.
A. Borzou, K. Call, J. Dittmann, K. Hatakeyama, H. Liu, N. Pastika

The University of Alabama, Tuscaloosa, U.S.A.
O. Charaf, S.I. Cooper, C. Henderson, P. Rumerio

Boston University, Boston, U.S.A.
D. Arcaro, A. Avetisyan, T. Bose, D. Gastler, D. Rankin, C. Richardson, J. Rohlf, L. Sulak, D. Zou

Brown University, Providence, U.S.A.
J. Alimena, G. Benelli, E. Berry, D. Cutts, A. Ferapontov, A. Garabedian, J. Hakala, U. Heintz, O. Jesus, E. Laird, G. Landsberg, Z. Mao, M. Narain, S. Piperov, S. Sagir, R. Syarif

JHEP10(2016)129

University of California, Davis, Davis, U.S.A.

R. Breedon, G. Breto, M. Calderon De La Barca Sanchez, S. Chauhan, M. Chertok, J. Conway, R. Conway, P.T. Cox, R. Erbacher, G. Funk, M. Gardner, J. Gunion, W. Ko, R. Lander, C. Mclean, M. Mulhearn, D. Pellett, J. Pilot, F. Ricci-Tam, S. Shalhout, J. Smith, M. Squires, D. Stolp, M. Tripathi, S. Wilbur, R. Yohay

University of California, Los Angeles, U.S.A.

R. Cousins, P. Everaerts, A. Florent, J. Hauser, M. Ignatenko, D. Saltzberg, E. Takasugi, V. Valuev, M. Weber

University of California, Riverside, Riverside, U.S.A.

K. Burt, R. Clare, J. Ellison, J.W. Gary, G. Hanson, J. Heilman, M. Ivova PANEVA, P. Jandir, E. Kennedy, F. Lacroix, O.R. Long, M. Malberti, M. Olmedo Negrete, A. Shrinivas, H. Wei, S. Wimpenny, B. R. Yates

University of California, San Diego, La Jolla, U.S.A.

J.G. Branson, G.B. Cerati, S. Cittolin, R.T. D'Agnolo, M. Derdzinski, A. Holzner, R. Kelley, D. Klein, J. Letts, I. Macneill, D. Olivito, S. Padhi, M. Pieri, M. Sani, V. Sharma, S. Simon, M. Tadel, A. Vartak, S. Wasserbaech[62], C. Welke, F. Würthwein, A. Yagil, G. Zevi Della Porta

University of California, Santa Barbara, Santa Barbara, U.S.A.

J. Bradmiller-Feld, C. Campagnari, A. Dishaw, V. Dutta, K. Flowers, M. Franco Sevilla, P. Geffert, C. George, F. Golf, L. Gouskos, J. Gran, J. Incandela, N. Mccoll, S.D. Mullin, J. Richman, D. Stuart, I. Suarez, C. West, J. Yoo

California Institute of Technology, Pasadena, U.S.A.

D. Anderson, A. Apresyan, J. Bendavid, A. Bornheim, J. Bunn, Y. Chen, J. Duarte, A. Mott, H.B. Newman, C. Pena, M. Spiropulu, J.R. Vlimant, S. Xie, R.Y. Zhu

Carnegie Mellon University, Pittsburgh, U.S.A.

M.B. Andrews, V. Azzolini, A. Calamba, B. Carlson, T. Ferguson, M. Paulini, J. Russ, M. Sun, H. Vogel, I. Vorobiev

University of Colorado Boulder, Boulder, U.S.A.

J.P. Cumalat, W.T. Ford, A. Gaz, F. Jensen, A. Johnson, M. Krohn, T. Mulholland, U. Nauenberg, K. Stenson, S.R. Wagner

Cornell University, Ithaca, U.S.A.

J. Alexander, A. Chatterjee, J. Chaves, J. Chu, S. Dittmer, N. Eggert, N. Mirman, G. Nicolas Kaufman, J.R. Patterson, A. Rinkevicius, A. Ryd, L. Skinnari, L. Soffi, W. Sun, S.M. Tan, W.D. Teo, J. Thom, J. Thompson, J. Tucker, Y. Weng, P. Wittich

Fermi National Accelerator Laboratory, Batavia, U.S.A.

S. Abdullin, M. Albrow, G. Apollinari, S. Banerjee, L.A.T. Bauerdick, A. Beretvas, J. Berryhill, P.C. Bhat, G. Bolla, K. Burkett, J.N. Butler, H.W.K. Cheung, F. Chlebana, S. Cihangir, V.D. Elvira, I. Fisk, J. Freeman, E. Gottschalk, L. Gray, D. Green, S. Grünendahl, O. Gutsche, J. Hanlon, D. Hare, R.M. Harris, S. Hasegawa, J. Hirschauer,

JHEP10(2016)129

Z. Hu, B. Jayatilaka, S. Jindariani, M. Johnson, U. Joshi, B. Klima, B. Kreis, S. Lammel, J. Lewis, J. Linacre, D. Lincoln, R. Lipton, T. Liu, R. Lopes De Sá, J. Lykken, K. Maeshima, J.M. Marraffino, S. Maruyama, D. Mason, P. McBride, P. Merkel, S. Mrenna, S. Nahn, C. Newman-Holmes†, V. O'Dell, K. Pedro, O. Prokofyev, G. Rakness, E. Sexton-Kennedy, A. Soha, W.J. Spalding, L. Spiegel, S. Stoynev, N. Strobbe, L. Taylor, S. Tkaczyk, N.V. Tran, L. Uplegger, E.W. Vaandering, C. Vernieri, M. Verzocchi, R. Vidal, M. Wang, H.A. Weber, A. Whitbeck

University of Florida, Gainesville, U.S.A.

D. Acosta, P. Avery, P. Bortignon, D. Bourilkov, A. Brinkerhoff, A. Carnes, M. Carver, D. Curry, S. Das, R.D. Field, I.K. Furic, J. Konigsberg, A. Korytov, K. Kotov, P. Ma, K. Matchev, H. Mei, P. Milenovic[63], G. Mitselmakher, D. Rank, R. Rossin, L. Shchutska, M. Snowball, D. Sperka, N. Terentyev, L. Thomas, J. Wang, S. Wang, J. Yelton

Florida International University, Miami, U.S.A.

S. Linn, P. Markowitz, G. Martinez, J.L. Rodriguez

Florida State University, Tallahassee, U.S.A.

A. Ackert, J.R. Adams, T. Adams, A. Askew, S. Bein, J. Bochenek, B. Diamond, J. Haas, S. Hagopian, V. Hagopian, K.F. Johnson, A. Khatiwada, H. Prosper, M. Weinberg

Florida Institute of Technology, Melbourne, U.S.A.

M.M. Baarmand, V. Bhopatkar, S. Colafranceschi[64], M. Hohlmann, H. Kalakhety, D. Noonan, T. Roy, F. Yumiceva

University of Illinois at Chicago (UIC), Chicago, U.S.A.

M.R. Adams, L. Apanasevich, D. Berry, R.R. Betts, I. Bucinskaite, R. Cavanaugh, O. Evdokimov, L. Gauthier, C.E. Gerber, D.J. Hofman, P. Kurt, C. O'Brien, I.D. Sandoval Gonzalez, P. Turner, N. Varelas, Z. Wu, M. Zakaria, J. Zhang

The University of Iowa, Iowa City, U.S.A.

B. Bilki[65], W. Clarida, K. Dilsiz, S. Durgut, R.P. Gandrajula, M. Haytmyradov, V. Khristenko, J.-P. Merlo, H. Mermerkaya[66], A. Mestvirishvili, A. Moeller, J. Nachtman, H. Ogul, Y. Onel, F. Ozok[67], A. Penzo, C. Snyder, E. Tiras, J. Wetzel, K. Yi

Johns Hopkins University, Baltimore, U.S.A.

I. Anderson, B.A. Barnett, B. Blumenfeld, A. Cocoros, N. Eminizer, D. Fehling, L. Feng, A.V. Gritsan, P. Maksimovic, M. Osherson, J. Roskes, U. Sarica, M. Swartz, M. Xiao, Y. Xin, C. You

The University of Kansas, Lawrence, U.S.A.

P. Baringer, A. Bean, C. Bruner, R.P. Kenny III, D. Majumder, M. Malek, W. Mcbrayer, M. Murray, S. Sanders, R. Stringer, Q. Wang

Kansas State University, Manhattan, U.S.A.

A. Ivanov, K. Kaadze, S. Khalil, M. Makouski, Y. Maravin, A. Mohammadi, L.K. Saini, N. Skhirtladze, S. Toda

JHEP10(2016)129

Lawrence Livermore National Laboratory, Livermore, U.S.A.

D. Lange, F. Rebassoo, D. Wright

University of Maryland, College Park, U.S.A.

C. Anelli, A. Baden, O. Baron, A. Belloni, B. Calvert, S.C. Eno, C. Ferraioli, J.A. Gomez, N.J. Hadley, S. Jabeen, R.G. Kellogg, T. Kolberg, J. Kunkle, Y. Lu, A.C. Mignerey, Y.H. Shin, A. Skuja, M.B. Tonjes, S.C. Tonwar

Massachusetts Institute of Technology, Cambridge, U.S.A.

A. Apyan, R. Barbieri, A. Baty, R. Bi, K. Bierwagen, S. Brandt, W. Busza, I.A. Cali, Z. Demiragli, L. Di Matteo, G. Gomez Ceballos, M. Goncharov, D. Gulhan, Y. Iiyama, G.M. Innocenti, M. Klute, D. Kovalskyi, K. Krajczar, Y.S. Lai, Y.-J. Lee, A. Levin, P.D. Luckey, A.C. Marini, C. Mcginn, C. Mironov, S. Narayanan, X. Niu, C. Paus, C. Roland, G. Roland, J. Salfeld-Nebgen, G.S.F. Stephans, K. Sumorok, K. Tatar, M. Varma, D. Velicanu, J. Veverka, J. Wang, T.W. Wang, B. Wyslouch, M. Yang, V. Zhukova

University of Minnesota, Minneapolis, U.S.A.

A.C. Benvenuti, B. Dahmes, A. Evans, A. Finkel, A. Gude, P. Hansen, S. Kalafut, S.C. Kao, K. Klapoetke, Y. Kubota, Z. Lesko, J. Mans, S. Nourbakhsh, N. Ruckstuhl, R. Rusack, N. Tambe, J. Turkewitz

University of Mississippi, Oxford, U.S.A.

J.G. Acosta, S. Oliveros

University of Nebraska-Lincoln, Lincoln, U.S.A.

E. Avdeeva, R. Bartek, K. Bloom, S. Bose, D.R. Claes, A. Dominguez, C. Fangmeier, R. Gonzalez Suarez, R. Kamalieddin, D. Knowlton, I. Kravchenko, F. Meier, J. Monroy, F. Ratnikov, J.E. Siado, G.R. Snow, B. Stieger

State University of New York at Buffalo, Buffalo, U.S.A.

M. Alyari, J. Dolen, J. George, A. Godshalk, C. Harrington, I. Iashvili, J. Kaisen, A. Kharchilava, A. Kumar, S. Rappoccio, B. Roozbahani

Northeastern University, Boston, U.S.A.

G. Alverson, E. Barberis, D. Baumgartel, M. Chasco, A. Hortiangtham, A. Massironi, D.M. Morse, D. Nash, T. Orimoto, R. Teixeira De Lima, D. Trocino, R.-J. Wang, D. Wood, J. Zhang

Northwestern University, Evanston, U.S.A.

S. Bhattacharya, K.A. Hahn, A. Kubik, J.F. Low, N. Mucia, N. Odell, B. Pollack, M.H. Schmitt, K. Sung, M. Trovato, M. Velasco

University of Notre Dame, Notre Dame, U.S.A.

N. Dev, M. Hildreth, C. Jessop, D.J. Karmgard, N. Kellams, K. Lannon, N. Marinelli, F. Meng, C. Mueller, Y. Musienko[36], M. Planer, A. Reinsvold, R. Ruchti, N. Rupprecht, G. Smith, S. Taroni, N. Valls, M. Wayne, M. Wolf, A. Woodard

JHEP10(2016)129

The Ohio State University, Columbus, U.S.A.

L. Antonelli, J. Brinson, B. Bylsma, L.S. Durkin, S. Flowers, A. Hart, C. Hill, R. Hughes, W. Ji, T.Y. Ling, B. Liu, W. Luo, D. Puigh, M. Rodenburg, B.L. Winer, H.W. Wulsin

Princeton University, Princeton, U.S.A.

O. Driga, P. Elmer, J. Hardenbrook, P. Hebda, S.A. Koay, P. Lujan, D. Marlow, T. Medvedeva, M. Mooney, J. Olsen, C. Palmer, P. Piroué, D. Stickland, C. Tully, A. Zuranski

University of Puerto Rico, Mayaguez, U.S.A.

S. Malik

Purdue University, West Lafayette, U.S.A.

A. Barker, V.E. Barnes, D. Benedetti, D. Bortoletto, L. Gutay, M.K. Jha, M. Jones, A.W. Jung, K. Jung, D.H. Miller, N. Neumeister, B.C. Radburn-Smith, X. Shi, I. Shipsey, D. Silvers, J. Sun, A. Svyatkovskiy, F. Wang, W. Xie, L. Xu

Purdue University Calumet, Hammond, U.S.A.

N. Parashar, J. Stupak

Rice University, Houston, U.S.A.

A. Adair, B. Akgun, Z. Chen, K.M. Ecklund, F.J.M. Geurts, M. Guilbaud, W. Li, B. Michlin, M. Northup, B.P. Padley, R. Redjimi, J. Roberts, J. Rorie, Z. Tu, J. Zabel

University of Rochester, Rochester, U.S.A.

B. Betchart, A. Bodek, P. de Barbaro, R. Demina, Y. Eshaq, T. Ferbel, M. Galanti, A. Garcia-Bellido, J. Han, O. Hindrichs, A. Khukhunaishvili, K.H. Lo, P. Tan, M. Verzetti

Rutgers, The State University of New Jersey, Piscataway, U.S.A.

J.P. Chou, E. Contreras-Campana, D. Ferencek, Y. Gershtein, E. Halkiadakis, M. Heindl, D. Hidas, E. Hughes, S. Kaplan, R. Kunnawalkam Elayavalli, A. Lath, K. Nash, H. Saka, S. Salur, S. Schnetzer, D. Sheffield, S. Somalwar, R. Stone, S. Thomas, P. Thomassen, M. Walker

University of Tennessee, Knoxville, U.S.A.

M. Foerster, G. Riley, K. Rose, S. Spanier, K. Thapa

Texas A&M University, College Station, U.S.A.

O. Bouhali[68], A. Castaneda Hernandez[68], A. Celik, M. Dalchenko, M. De Mattia, A. Delgado, S. Dildick, R. Eusebi, J. Gilmore, T. Huang, T. Kamon[69], V. Krutelyov, R. Mueller, I. Osipenkov, Y. Pakhotin, R. Patel, A. Perloff, D. Rathjens, A. Rose, A. Safonov, A. Tatarinov, K.A. Ulmer

Texas Tech University, Lubbock, U.S.A.

N. Akchurin, C. Cowden, J. Damgov, C. Dragoiu, P.R. Dudero, J. Faulkner, S. Kunori, K. Lamichhane, S.W. Lee, T. Libeiro, S. Undleeb, I. Volobouev

JHEP10(2016)129

Vanderbilt University, Nashville, U.S.A.

E. Appelt, A.G. Delannoy, S. Greene, A. Gurrola, R. Janjam, W. Johns, C. Maguire, Y. Mao, A. Melo, H. Ni, P. Sheldon, S. Tuo, J. Velkovska, Q. Xu

University of Virginia, Charlottesville, U.S.A.

M.W. Arenton, P. Barria, B. Cox, B. Francis, J. Goodell, R. Hirosky, A. Ledovskoy, H. Li, C. Neu, T. Sinthuprasith, X. Sun, Y. Wang, E. Wolfe, J. Wood, F. Xia

Wayne State University, Detroit, U.S.A.

C. Clarke, R. Harr, P.E. Karchin, C. Kottachchi Kankanamge Don, P. Lamichhane, J. Sturdy

University of Wisconsin - Madison, Madison, WI, U.S.A.

D.A. Belknap, D. Carlsmith, S. Dasu, L. Dodd, S. Duric, B. Gomber, M. Grothe, M. Herndon, A. Hervé, P. Klabbers, A. Lanaro, A. Levine, K. Long, R. Loveless, A. Mohapatra, I. Ojalvo, T. Perry, G.A. Pierro, G. Polese, T. Ruggles, T. Sarangi, A. Savin, A. Sharma, N. Smith, W.H. Smith, D. Taylor, P. Verwilligen, N. Woods

†: Deceased
1: Also at Vienna University of Technology, Vienna, Austria
2: Also at State Key Laboratory of Nuclear Physics and Technology, Peking University, Beijing, China
3: Also at Institut Pluridisciplinaire Hubert Curien, Université de Strasbourg, Université de Haute Alsace Mulhouse, CNRS/IN2P3, Strasbourg, France
4: Also at Universidade Estadual de Campinas, Campinas, Brazil
5: Also at Centre National de la Recherche Scientifique (CNRS) - IN2P3, Paris, France
6: Also at Université Libre de Bruxelles, Bruxelles, Belgium
7: Also at Laboratoire Leprince-Ringuet, Ecole Polytechnique, IN2P3-CNRS, Palaiseau, France
8: Also at Joint Institute for Nuclear Research, Dubna, Russia
9: Also at Ain Shams University, Cairo, Egypt
10: Also at Fayoum University, El-Fayoum, Egypt
11: Now at British University in Egypt, Cairo, Egypt
12: Also at Université de Haute Alsace, Mulhouse, France
13: Also at CERN, European Organization for Nuclear Research, Geneva, Switzerland
14: Also at Skobeltsyn Institute of Nuclear Physics, Lomonosov Moscow State University, Moscow, Russia
15: Also at Tbilisi State University, Tbilisi, Georgia
16: Also at RWTH Aachen University, III. Physikalisches Institut A, Aachen, Germany
17: Also at University of Hamburg, Hamburg, Germany
18: Also at Brandenburg University of Technology, Cottbus, Germany
19: Also at Institute of Nuclear Research ATOMKI, Debrecen, Hungary
20: Also at MTA-ELTE Lendület CMS Particle and Nuclear Physics Group, Eötvös Loránd University, Budapest, Hungary
21: Also at University of Debrecen, Debrecen, Hungary
22: Also at Indian Institute of Science Education and Research, Bhopal, India
23: Also at University of Visva-Bharati, Santiniketan, India
24: Now at King Abdulaziz University, Jeddah, Saudi Arabia

JHEP10(2016)129

25: Also at University of Ruhuna, Matara, Sri Lanka
26: Also at Isfahan University of Technology, Isfahan, Iran
27: Also at University of Tehran, Department of Engineering Science, Tehran, Iran
28: Also at Plasma Physics Research Center, Science and Research Branch, Islamic Azad University, Tehran, Iran
29: Also at Università degli Studi di Siena, Siena, Italy
30: Also at Purdue University, West Lafayette, U.S.A.
31: Now at Hanyang University, Seoul, Korea
32: Also at International Islamic University of Malaysia, Kuala Lumpur, Malaysia
33: Also at Malaysian Nuclear Agency, MOSTI, Kajang, Malaysia
34: Also at Consejo Nacional de Ciencia y Tecnología, Mexico city, Mexico
35: Also at Warsaw University of Technology, Institute of Electronic Systems, Warsaw, Poland
36: Also at Institute for Nuclear Research, Moscow, Russia
37: Now at National Research Nuclear University 'Moscow Engineering Physics Institute' (MEPhI), Moscow, Russia
38: Also at St. Petersburg State Polytechnical University, St. Petersburg, Russia
39: Also at California Institute of Technology, Pasadena, U.S.A.
40: Also at Faculty of Physics, University of Belgrade, Belgrade, Serbia
41: Also at INFN Sezione di Roma; Università di Roma, Roma, Italy
42: Also at National Technical University of Athens, Athens, Greece
43: Also at Scuola Normale e Sezione dell'INFN, Pisa, Italy
44: Also at National and Kapodistrian University of Athens, Athens, Greece
45: Also at Institute for Theoretical and Experimental Physics, Moscow, Russia
46: Also at Albert Einstein Center for Fundamental Physics, Bern, Switzerland
47: Also at Adiyaman University, Adiyaman, Turkey
48: Also at Mersin University, Mersin, Turkey
49: Also at Cag University, Mersin, Turkey
50: Also at Piri Reis University, Istanbul, Turkey
51: Also at Gaziosmanpasa University, Tokat, Turkey
52: Also at Ozyegin University, Istanbul, Turkey
53: Also at Izmir Institute of Technology, Izmir, Turkey
54: Also at Marmara University, Istanbul, Turkey
55: Also at Kafkas University, Kars, Turkey
56: Also at Istanbul Bilgi University, Istanbul, Turkey
57: Also at Yildiz Technical University, Istanbul, Turkey
58: Also at Hacettepe University, Ankara, Turkey
59: Also at Rutherford Appleton Laboratory, Didcot, United Kingdom
60: Also at School of Physics and Astronomy, University of Southampton, Southampton, United Kingdom
61: Also at Instituto de Astrofísica de Canarias, La Laguna, Spain
62: Also at Utah Valley University, Orem, U.S.A.
63: Also at University of Belgrade, Faculty of Physics and Vinca Institute of Nuclear Sciences, Belgrade, Serbia
64: Also at Facoltà Ingegneria, Università di Roma, Roma, Italy
65: Also at Argonne National Laboratory, Argonne, U.S.A.
66: Also at Erzincan University, Erzincan, Turkey
67: Also at Mimar Sinan University, Istanbul, Istanbul, Turkey
68: Also at Texas A&M University at Qatar, Doha, Qatar
69: Also at Kyungpook National University, Daegu, Korea

JHEP10(2016)129